Proceedings of the

# 7th Oxford Tidal Energy Workshop

8 - 9 April 2019, Oxford, UK


# *Proceedings of the 7th Oxford Tidal Energy Workshop (OTE 2019)*

8-9 April 2019, Oxford, UK

## Monday 8th April

### Session 1: Device modelling and performance (1)



### Poster Presentations



### Session 2: Environmental and resource modelling



### Session 3: Experimental testing





EPSRC Engineering and Physical Sciences Research Council
UNIVERSITY OF OXFORD

## Tuesday 9th April

### Session 4: Floating platform dynamics



### Session 5: Array modelling and control



### Session 6: Device modelling and performance (2)



### Workshop Organisers:

| | | |
|---|---|---|
| Richard H. J. Willden | (Chairman) | University of Oxford |
| Christopher R. Vogel | (Co-Chairman) | University of Oxford |

### Scientific Committee Members:

| | | | |
|---|---|---|---|
| T. A. A. Adcock | (University of Oxford) | J. Thake | (SIMEC Atlantis Energy) |
| G. T. Houlsby | (University of Oxford) | I. M. Viola | (University of Edinburgh) |
| I. Masters | (Swansea University) | C. R. Vogel | (University of Oxford) |
| T. Nishino | (University of Oxford) | R. H. J. Willden | (University of Oxford) |
| T. Stallard | (University of Manchester) | | |

### Sponsor:


Engineering and Physical Sciences Research Council

# An adaptive 3D force distribution model for calculating interactions and power production in an array of vertical axis water turbines

Clary V.*, Delafin P.L., Maitre T.
*Univ. Grenoble Alpes, Grenoble INP[1], LEGI, 38000 Grenoble, France*
[1]*Institute of Engineering Univ. Grenoble Alpes*
Oudart T.
*Artelia Eau & Environnement, 38130 Echirolles, France*

*Summary:* A simplified steady state CFD model using force source terms is implemented in OpenFoam to model the power production and the flow in an array of vertical axis tidal turbines. The study explains how to interpolate the force distributions from a set of blade resolved simulations of a whole turbine, depending on the flow striking each turbine of the array.

## Introduction

Modeling wind, river or tidal turbine wake interactions between several machines is challenging because the physics in the wake must be modeled with a sufficient accuracy, yet not too much details to keep large array simulations affordable. Simplified CFD models have therefore been developed, using force source terms to represent the action of the turbine on the flow. An example of such model for vertical axis turbines is the Actuator Line model coupled to a LES solver developed by Mendoza et al.[1]. The model takes into account the dynamic stall to obtain the drag and lift curves providing the forces to apply, and gives excellent results. The approach developed here is even more simplified and uses affordable steady state simulations, with a detailed force distribution.

## Methods

The simplified model developed in this work uses steady state RANS simulations and represents vertical axis turbines by an average force distribution. This force distribution is obtained beforehand from unsteady blade-resolved simulations of one whole turbine (3D URANS simulations) and it is therefore varying with the azimuth angle. The simplified model uses the k-omega SST turbulence model and has been validated by a comparison to experiments [2]. It proves to give good results for modeling the far wake (further than 4 diameters downstream of the turbine) but poor accuracy in the near wake. This is considered sufficient for modeling turbine arrays, where distances between consecutive turbines are expected to be bigger than this value.

In a turbine array, the forces to impose must be calculated depending on the flow velocity striking each turbine. The local machine velocity, named $U_{local}$, is obtained with a spatial-averaging of the velocity in all cells of the cylinder swept by the vertical axis turbine, as shown in Figure 1.a. A local advance parameter $\lambda^* = (\Omega R)/U_{local}$ can be defined using this local velocity (with R the radius and $\Omega$ the rotational speed of the turbine). The power coefficient curves drawn using the velocity far upstream of the turbine give different results depending on the confinement of the turbine used. It seems that results become independent of the confinement when using the local machine velocity to compute the corresponding power coefficient $C_p^*$ as a function of $\lambda^*$. Local force coefficients for each components of force (the thrust coefficient and the equivalent coefficients in the 2 other directions) can be defined in the same way, and also seem to be independent of the confinement used. Although not shown here, this phenomenon is verified by comparing three different confinement cases of blade resolved URANS simulations.

In the adaptative force distribution model, forces added in the momentum equations are calculated at each iteration. The local machine velocity is calculated, then the corresponding forces are interpolated from the force coefficient curves obtained before with a set of blade resolved calculations. The rotational speed of the machine $\Omega$, or a certain value of $\lambda^*$, can be chosen to impose the operating point of each turbine depending on the control strategy chosen. After convergence, the power produced by each turbine is calculated with the power coefficient curve depending on the local machine velocity. All those steps are summarized in Figure 1.b.

## Results

A configuration of 5 vertical axis turbines placed in a confined channel is tested and presented in Figure 2. The constant $\lambda^*$ control strategy is used, therefore the turbines rotate at different speeds (see Table 1). To be

*Corresponding author.
*Email address:* vincent.clary@univ-grenoble-alpes.fr

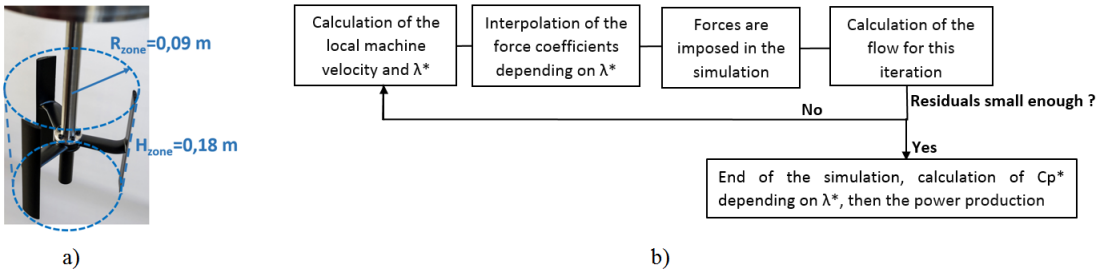


Figure 1: a) Volume used for the local velocity calculation; b) Computation loop of the force distribution model

dimensionless, the output power is divided by the nominal power generated by the same turbine in unconfined conditions, at its point of maximum efficiency. We can see in Table 1 that the power productions of the turbines located on both sides of the first turbine benefit from the acceleration of the fluid created on both sides of its wake. The turbine 1 located approximately 8.5 diameters downstream of turbine 0 witnesses a power reduction, and turbine 4 located too close to turbine 1 (3.5 diameters downstream) has a drastic reduction in power production.

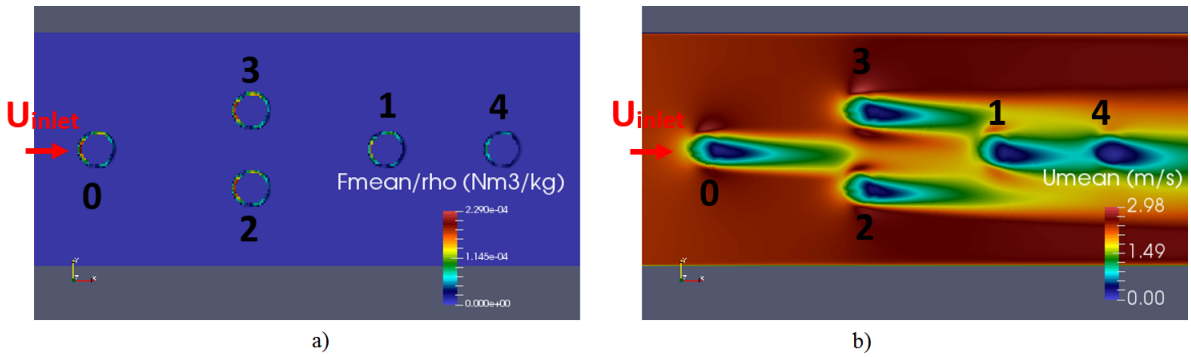


Figure 2: a) Norm of the force distributions; and b) Velocity field; in a horizontal plane crossing the turbine blades

| Turbine number | 0 | 1 | 2 | 3 | 4 |
|---|---|---|---|---|---|
| P /$P_n$ | 0.97 | 0.60 | 1.10 | 1.11 | 0.23 |
| $\lambda^*$ | 3.51 | 3.51 | 3.51 | 3.51 | 3.51 |
| $\Omega$ (rad/s) | 47.5 | 40.4 | 49.5 | 49.8 | 29.5 |

Table 1: Operating values $\Omega$ and $\lambda^*$, and dimensionless power production of each turbine

## Conclusions

Promising results are obtained using the presented method to adapt the force distribution to the local velocity of each turbine, and the behavior of turbines in an array is reproduced correctly. The convergence loop proves to be stable even for unfavorable cases with a turbine placed in the near-wake of another one. Results are however qualitative and different settings (mesh convergence, etc...) or configurations still need to be tested.

*Acknowledgments:*
This work is part of the ANR 3DMMTA project funded by the french "Agence nationale de la recherche". Part of the simulation results were obtained with the help of the CIMENT calculation mesocenter at Grenoble.

*References:*

[1] Mendoza V., Bachant P., Ferreira C., Goude A. *Near-wake flow simulation of a vertical axis turbine using an actuator line model*, Wind Energy 2019; 22:171-188.

[2] Clary V., Oudart T., Maitre T., Sommeria J. et al. *A simple 3D river/tidal turbine model for farm computation - Comparison with experiments*, Sixth International Conference on Estuaries and Coasts, August 20-23, 2018, Caen, France; hal-01897925

# Preliminary assessment of blade twist-deformation as a load relief mechanism for tidal turbine blades

Federico Zilic de Arcos*, Christopher Vogel, Richard H. J. Willden
*Department of Engineering Science, University of Oxford, Oxford, UK*

*Summary:* This work presents a preliminary assessment of the effect of blade twist deformations as part of a turbine control strategy to alleviate blade loading. The analysis starts by presenting blade-resolved CFD simulation results supporting twist-deformation as the biggest component on the thrust loading distribution at different tip-speed ratios and continues by using blade-element momentum theory to explore the potential for, and deformations required to obtain the necessary load relief that could be used in place of mechanically-complex blade-pitching mechanisms.

## Introduction

Blade deflections can be described as a linear superposition of three different deformations: flapwise, edgewise and twist. These three components affect the hydrodynamic performance and loading of turbines in different ways, and the underlying physics of these effects is not presently well understood.

The analysis presented herein is based on a 10m radius tidal turbine designed for blocked flow conditions (Blockage, B = 0.197) [1][2]. Using the hydroelastic model and the structural design described in [3], blade deformations were computed for three different tip-speed ratios (4.0, 5.5 and 7.0) at a flow-speed of 4.5 m/s in unblocked flow conditions. These deformations, based on the displacement of the quarter-chord line were used to define the deformed blade geometries and subsequently perform a set of blade-resolved CFD simulations that allowed an analysis of the decoupled hydrodynamic effects due to each deformation component.

The results of the blade resolved CFD simulations suggested that the dominant hydroelastic deformation is twist. Blade Element Momentum (BEM) theory [4] was used here to obtain a preliminary analysis of the possibilities and limitations of using passive deformations as part of a turbine control strategy with the aim of replacing mechanically complex blade-pitching mechanisms.

## Blade-resolved CFD analysis of the deformation mechanisms

Fluent 19.0 was employed to perform blade-resolved steady-state RANS simulations [5] using the $k-\omega$ SST turbulence model [6] of the different deformation cases. Azimuthal symmetry of the problem was exploited by modelling a 120º wedge and using periodic boundary conditions. The domain was separated in two regions and a moving reference frame approach was employed. Structured meshes of approximately 4.5 million elements were prepared for every case using ICEM 18.2, and the non-dimensional wall distance $Y^+$was kept within the wall-modelling region ($30 \geq Y^+ \geq 300$).

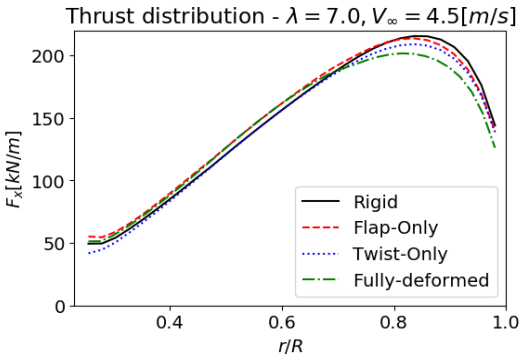


Fig. 1. Thrust distribution over the blade at a TSR of 7.0 and a flow speed of 4.5 [m/s]

Representative results from the CFD simulations for a tip-speed ratio of 7.0 are shown in Fig. 1 where the thrust force distributions of the undeformed blade, the fully-deformed blade and the blade considering only flapwise and only twist deformations are shown for a flow speed of 4.5m/s. The results show that even a limited angular deformation (less than 1° at the tip) can cause a significant influence on overall loads, especially near the tip, whereas the flapwise deformation, being about 0.5m at tip, has a limited effect on loads over the blade. Following these results, a preliminary assessment of the effects of twist deformation based on BEM theory is introduced in the next section.

## Exploratory analysis of twist deformations

This preliminary assessment was performed using BEM theory to analyse different cases of assumed twist deformation. The twist deformations, which were used as input to the BEM model, were prescribed over the rotor by a simplified model. The deformations are added to the original twist distribution $\beta(r)$ as a linear function, being

* Corresponding author.
*Email address*: federico.zilic@eng.ox.ac.uk

0 at the root and having a maximum value of $\delta\beta_{max}$ at the tip. This maximum deformation is further assumed to be proportional to the square of the flow-speed in the form of $\delta\beta_{max} = F \cdot V_\infty^2$, with $F$ the proportionality factor and $V_\infty$ the undisturbed flow velocity. Using this model of blade flexibility, we analyse passive control of the rotor, which is additionally assumed to have variable rotational speed over the flow speed range 0 to 5m/s. With those constraints, the objective of the control strategy was to maximise power extraction from the cut-in to the rated design speed (2 m/s), and then maintaining the rated power from the design to the cut-out speed (5 m/s).

Three different flexibility factors $F$ were tested: 15/25, 30/25 and 45/25, exhibiting maximum deformations of 15°, 30° and 45° at the tip respectively at a flow-speed of 5 m/s. In addition, a variable-speed rigid-blade turbine is provided for reference; see Fig. 2. By using a combination of overspeed control (limiting the maximum tip-speed ratio to 10) and passive blade deformation, non-stall control paths can be mapped out for each blade flexibility. Through these, power can be maintained at target across the desired flow speed range, with somewhat reduced thrust loads, although less than could be achieved with an active pitch mechanism which would see reduced loads above rated.

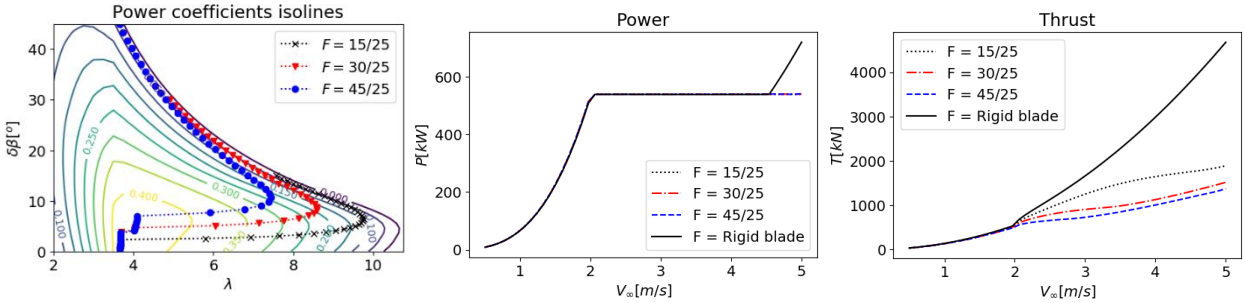


Fig. 2. BEM analysis of flexible blades. Displayed, from left to right, the control path over the power coefficient isosurface, the power and the thrust curves for three different flexibilities (15/25, 30/25 and 45/25). Rigid-blade fixed-speed turbine results are also provided for comparison.

## Conclusions

Twist deformations appear to have the largest effect on the hydrodynamic performance of turbine blades. Utilising the loading changes associated with blade deformations, along with appropriate control strategies, it is possible to effectively achieve a fixed rated power. However, large deformations are required to maintain the velocity control within sensible limits (e.g. to avoid cavitation). The magnitude of deformations is dependent on the ratio of rated to cut-out flow speed. Furthermore, large increases in thrust may be detrimental to blade structural design. This is principally a result of operating the deformed turbine at higher tip-speed ratios to avoid stall.

*Acknowledgements:*

The first author would like to acknowledge the support of CONICYT PFCHA/BECAS CHILE DOCTORADO EN EL EXTRANJERO 2016 /72170292.
The authors would also like to acknowledge the use of the University of Oxford Advanced Research Computing (ARC) facility in carrying out this work. http://dx.doi.org/10.5281/zenodo.22558

*References:*

[1] Schluntz, J., & Willden, R. H. J. (2015). The effect of blockage on tidal turbine rotor design and performance. Renewable energy, 81, 432-441.
[2] Wimshurst, A., & Willden, R. H. J. (2016). Computational analysis of blockage designed tidal turbine rotors. In Progress in Renewable Energies Offshore: Proceedings of the 2nd International Conference on Renewable Energies, 2016 (RENEW2016) (pp. 587-597). Taylor & Francis Books Ltd.
[3] Zilic de Arcos, F., Vogel, C. & Willden, R. H. J. (2018). Hydroelastic modelling of composite tidal turbine blades. In Advances in Renewable Energies Offshore: Proceedings of the 3rd International Conference on Renewable Energies Offshore (RENEW 2018), October 8-10, 2018, Lisbon, Portugal (p. 137). CRC Press.
[4] Ning, S. A. (2014). A simple solution method for the blade element momentum equations with guaranteed convergence. Wind Energy, 17(9), 1327-1345.
[5] Ansys Inc. (2018). ANSYS FLUENT Theory Guide (Release 19.0).
[6] Menter, F. R. (1994). Two-equation eddy-viscosity turbulence models for engineering applications. AIAA journal, 32(8), 1598-1605.

# Investigating the Hydrokinetic Turbine wake effects as a result of operational parameter variations through validated CFD models

Chantel Niebuhr*, Marco van Dijk
*Department of Civil Engineering, University of Pretoria, South Africa*

Christiaan de Wet
*Aerotherm Computational Dynamics, South Africa*

*Summary:* Hydrokinetic energy generation devices within water infrastructure are becoming an ever-increasing alternative power source. In these applications the extent and characteristics of the downstream wake are of great importance. The vortex formation and diffusion of the wake has a complex formation and is dependent on numerous factors. Validated Computational Fluid Dynamics (CFD) models provide a detailed insight into these formations. These models allow analysis of the wake behaviour as a result of changes in device operational characteristics which may be helpful to optimise installations, specifically in array applications. To test the applicability of CFD models and further understand the wake vortex formation, the tip speed ratio of a validated turbine model was varied and the changes in the downstream wake analysed.

## Introduction

Hydrokinetic (HK) devices placed in canals can have significant water level and hydrodynamic energy loss effects. Comprehension of the flow behaviour in the near and far wake for any specific HK device remains uncertain. The downstream disturbances from a HK turbine are characterised by intense turbulent mixing, helical movements and a complex eddy system defined as the wake [1]. Much of the wake complexity arises from an adverse pressure gradient at the rotor plane. Additionally, a spiral vortex structure is shed outwards from the blade tips producing large eddy structures which last a distance downstream. The eddy size, shape and behaviour vary with changes in impeller rotation rate. This flow behaviour may be identified by vortex shedding and results in non-uniformities in the velocity field [2]. The extent of this behaviour is not well understood or quantifiable as yet. From similar studies on wind turbine wake dissipation, the wake characteristics are defined as velocity deficit downstream and turbulence levels [3]. However, additional parameters such as the vorticity magnitude, determined from the curl and magnitude of the wake velocity vectors, may provide distinct characterisation and visualisation of the flow movement and extent of turbulence present in the wake.

## Methods

To allow further understanding of the wake behaviour at different TSRs (tip speed ratios) the RM1 axial flow duo-turbine was simulated in Siemens PLM Simcenter STAR-CCM+ commercial simulation software with a domain size and dimensions similar to the experimental results from the RM1 reference model turbine [4]. The Reynolds Averaged Navier Stokes (RANS) approach was adopted and the K-ω Shear-Stress Transport (SST) model was employed. The SST model has been found to give results for wall-bound flows even in highly separated regions (as typically found in axial turbines) [5, 6]. A polyhedral cell type was used to capture the fine wake dynamics and gradients. A mesh independence study was fulfilled to obtain the final mesh size required. Mesh refinements around the blades and in the turbulent wake region were employed, with care taken to ensure gradual mesh size growth. The finest mesh resulted in a minimum cell size of 3.5 mm.

A 2-part validation study was completed after model convergence, initially the turbine torque was calculated through fluid force moments about the rotational axis and compared to experimental results (Fig. 1). Furthermore, the time-averaged horizontal and vertical velocity profiles were compared to experimental results. The inlet velocity was 1.05 m/s with blade chord length Reynolds number = $3x10^5$. To allow further understanding of the wake behaviour and spiral vortex structure downstream of an axial HK device, the rotation rate was varied over 5 TSR's within the operational range (with torque measurement validation with each variation as shown in Fig 1). The vorticity profiles, as well as the vortex structure were recorded.

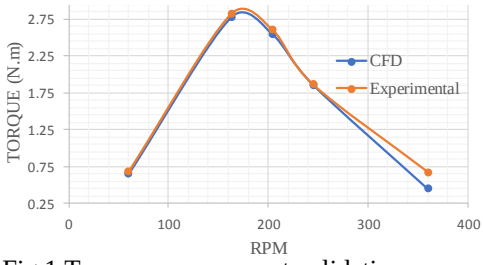

Fig 1.Torque measurement validation

* Corresponding author.
*Email address*: Chantel.niebuhr@up.ac.za

## Results

The vortex shedding and uneven wake distribution of the turbine operating at lower TSRs are prevalent in the vorticity plot (Fig 2). At higher TSRs, the effect of vortex shedding is minimized with concentrated rotational vortices dissipating uniformly downstream. The vortex shedding effect results in higher flow instabilities in the near wake which may be unfavourable to turbines placed in this zone. However, the turbulence dissipation and velocity deficit are lower at these TSRs. When normalized velocity is displayed, (Fig 2) the flow recovery profile is portrayed and indicates higher velocity changes in the near wake at higher TSRs. Compared to the RM1 experimental analysis, power output from scenario (b) and (d) has similar values to the simulated results with only a 0.03 difference in power co-efficient compared to scenario (c).

## Conclusions

The use of validated CFD models allows further understanding and visualisation into wake behaviour and vortex formation. This is specifically relevant in the case of HK conveyance infrastructure installation where the wake dynamics and downstream velocity deficit play a key role. Performing analysis on validated CFD models allows clear visualisation and understanding of the wake behaviour at specific operation parameters (TSR, inflow velocity, etc.) and may allow development of simplified relationships to quantify the wake extent and dissipation rate for any specific installation. Although, quantifying the wake as a function of TSR is a complex task due to the eddy formation and vortex shedding which is more prevalent at lower TSRs.

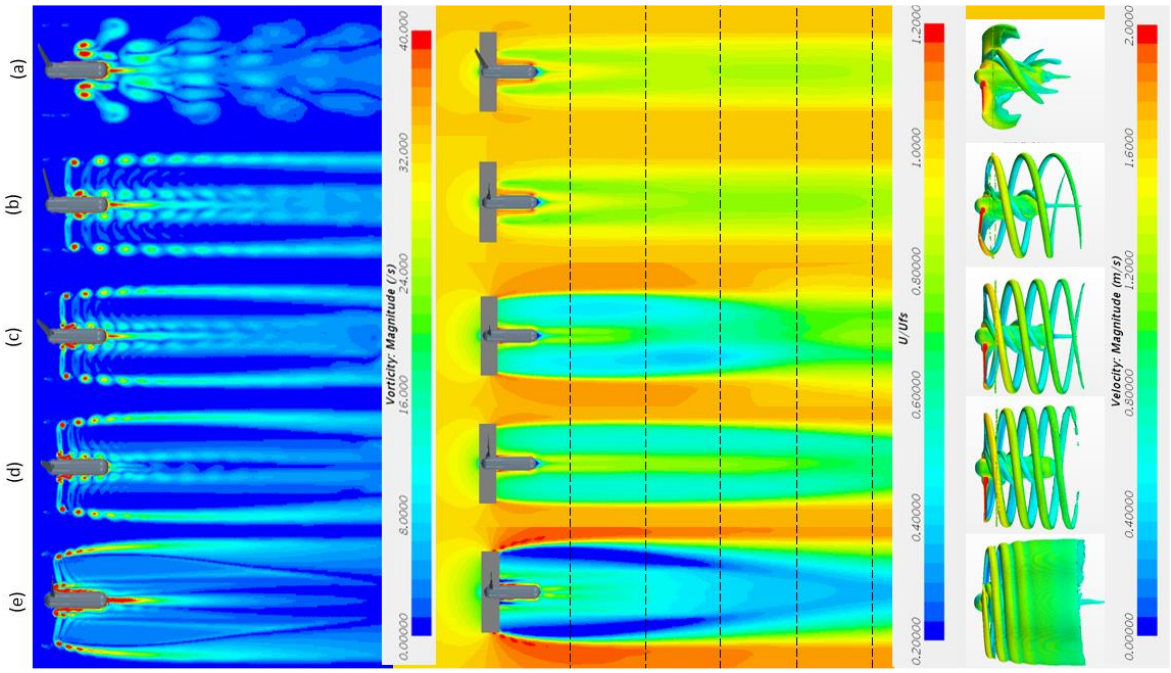


Fig. 2. Vorticity, mean normalized velocity and vortex profiles of a single RM1 turbine with a TSR of (a) 1.5 (b) 4.2 (c) 5.1 (d) 6.2 and (e) 9.1 and Cp (a)0.04 (b)0.45 (c)0.48 (d)0.45 and (e)0.23.

*Acknowledgements:*

The studies were completed through the University of Pretoria, South Africa, with help from Aerotherm's CFD specialists. The Centre for High Performance Computing (CHPC) was used for solving.

*References:*

[1] Silva P. A. S. F., Oliveira T. F. D. E., Junior A. C. P. B., Vaz J. R. P. (2016) Numerical Study of Wake Characteristics in a Horizontal-Axis Hydrokinetic Turbine. *Ann Brazilian Acad Sci*, **88**, 2441–2456.

[2] Seyed-aghazadeh B (2015) An experimental investigation of vortex-induced vibration of a rotating circular cylinder in the crossflow direction. *Physics of Fluids.*

[3] Chamorro LP, Porté-agel F (2009) A Wind-Tunnel Investigation of Wind-Turbine Wakes: Boundary-Layer Turbulence Effects. *Boundary-Layer Meteorol* **132**,129–149.

[4] Hill C, Neary VS, Gunawan B, Guala M, Sotiropoulos F (2014) U. S. Department of Energy Reference Model Program RM1: Experimental Results. Minneapolis.

[5] Moshfeghi M, Song YJ, Xie YH (2012) Effects of near-wall grid spacing on SST K-w model using REL Phase VI horizontal axis wind turbine. *J Wind Eng Ind Aerodyn* **107**, 94–105.

[6] Menter FR, Kuntz M, Langtry R (2003) Ten years of industrial experience with the SST turbulence model. *Turbul Heat Mass Transf* **4**, 625–632.

# Using 3D coastal tidal models to assess tidal array performance

Mohammed A. Almoghayer* and David K. Woolf
*International Centre for Island Technology, Heriot-Watt University, UK*

*Summary:* Two-dimensional (2D) depth-averaged simulations are used to investigate the performance of tidal turbine arrays. However, those models are incapable of taking into account the effects of the vertical position of the turbine on its performance. Results suggest that optimising the vertical position of the turbines is as important as optimising the horizontal configuration of the tidal array. 3D models provide a comprehensive tool to assess tidal array performance more realistically.

## Introduction

Various numerical methods such as CFD, BEM and RANS models have been used to study the interaction between tidal turbines and the tidal flow, and to investigate the performance of the tidal turbines. However, most of these studies consider idealised cases that cannot easily be translated to unsteady and non-uniform flow through a real channel [1]. Coastal tidal models provide an efficient and comprehensive approach to simulate tidal stream arrays in more realistic conditions. On the other hand, most of the studies which adopt this approach rely on 2D depth-averaged simulations to assess the performance of different tidal array layouts. 2D models ignore the effects of the turbine's vertical position in the water column and the close proximity to the seabed or the surface on the overall performance.

## Methods

TELEMAC-MASCARET modelling system is used to simulate unsteady and non-uniform flow through Hoy Sound in the Orkney Islands. A tidal array in form of partial tidal fence of 26 turbines that occupies a fraction of the channel width was selected for this study. Tidal turbines are represented in the TELEMAC-2D as a drag force (similar to increasing the seabed friction) using DRAGFO subroutine. The drag force is applied as a friction stress spread out over an area representing the turbine. This area is defined as the sum of the area of the nodes inside the turbine envelope [2]. Building on this approached, we developed a code to capture the effects of the drag force, which is exerted by the turbines on the flow, and apply it as a head loss in TELEMAC-3D. This stress is treated as a source term in the shallow water equations (more details about TELEMAC theoretical aspects can be found in [3]).

$$S_0 = Q = \frac{\tau_D}{\rho h} = -\frac{1}{2}\frac{\pi R^2}{Ah} C_D U_r |U_r|$$ ; where $S_0$ is the source term,

R is the radius of the rotor, A is the area affected by the drag force, $C_D$ is the drag coefficient, and $U_r$ is the undisturbed flow velocity upstream the turbine.

The location and size of the array were dictated by the availability of suitable depth and strong tidal flow. The cut-in speed is assumed 0.1 m/s and no upper limit for the cut-out speed. Also, the turbines are assumed to operate bi-directionally. The rotor diameter is 6m which was chosen to achieve the optimal depth ratio 3.5R [4], the power coefficient Cp is assumed 35%, and the drag coefficient Cd=1.2 which was found an appropriate value to reflect the impact of the presence of the turbines on the flow.

To better represent the tidal flow and capture the turbines wake without increasing the computational cost, the model was constructed with four different resolution scales. The average resolution of the wider model is 150m, then the resolution is increased gradually to 30m around Hoy Sound and 5m for the middle of the channel. The resolution of the farm area was increased to 1m.

The turbines were spaced at 0.5D tip-to-tip clearance, which achieves on average 12% global blockage ratio. Although this value does not reflect a high blockage ratio, the shape of the channel geometry and the spatial distribution of the flow amplify the effects of the blockage. On the other hand, the average local blockage in this arrangement is reasonably high at 29%.

* Corresponding author.
*Email address*: ma211@hw.ac.uk

To demonstrate and assess the effects of the turbine's position within the water column on its performance, the 3D simulation was run for two cases: a) turbines positioned at 4.5m depth and b) turbines positioned at 7.5m depth.

## Results

The simulation results show that the average power generated by the array in case (a) is ~7.68MW, while the array in case (b) generated ~8.14MW. This means that by just changing the depth of the turbines from 4.5m to 7.5m increased the power output by ~5%.

The effect of the presence of the turbines on the flow is illustrated in Fig. 1 & Fig. 2. The figures show clearly that turbines deployed at different depths will have a different impact on the flow. It will not just shift the same effects to the new depth, but it will create a different impact as observed by Kolekar & Banerjee [4]. They observed that the vertical position of the turbine and the proximity to the free surface add more complexity to the flow structure and affect the turbine efficiency. Those effects cannot be captured by 2D models.

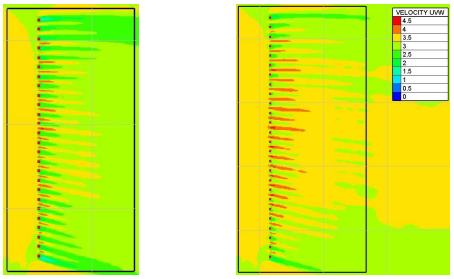


(a) (b)

Fig. 1. Simulation results at 4.5m depth.
(a) The turbines were deployed at 4.5m
(b) The turbines were deployed at 7.5m

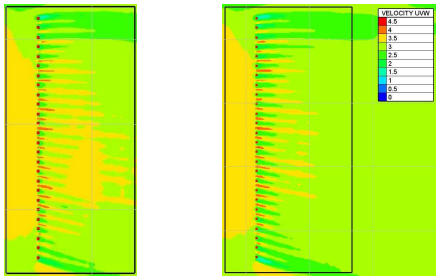


(a) (b)

Fig. 2. Simulation results at 7.5m depth.
(a) The turbines were deployed at 4.5m
(b) The turbines were deployed at 7.5m

## Conclusions

In this abstract, 3D simulations are used to investigate the impact of the vertical position of tidal turbines within the water column on its performance. At present, the existing tidal stream turbines technologies vary from seabed mounted to submerged and floating devices. This variation needs to be better captured and reflected in tidal arrays design and turbines performance assessment studies. 2D depth-averaged models are incapable of meeting this need. Contrary to 2D models, 3D models can better represent the various technologies and provide a more robust tool to assess tidal array performance.

*Acknowledgements:*

This paper is based on part of the first author's PhD study, which is sponsored by the Energy Technology Partnership ETP and Aquatera Ltd.

*References:*

[1] I. Masters, R. Malki, A. J. Williams, and T. N. Croft, "The influence of flow acceleration on tidal stream turbine wake dynamics: A numerical study using a coupled BEM–CFD model," *Appl. Math. Model.*, vol. 37, no. 16–17, pp. 7905–7918, Sep. 2013.

[2] A. Joly, C.-T. Pham, M. Andreewsky, S. Saviot, and L. Fillot, "Using the DRAGFO subroutine to model Tidal Energy Converters in Telemac-2D," in *XXII TELEMAC-MASCARET User Conference*, 2015, pp. 182–189.

[3] A. Leroy, "TELEMAC-3D: theory guide." 2018.

[4] N. Kolekar and A. Banerjee, "Performance characterization and placement of a marine hydrokinetic turbine in a tidal channel under boundary proximity and blockage effects," *Appl. Energy*, vol. 148, pp. 121–133, Jun. 2015.

# Optimising the Income of a Fleet of Tidal Lagoons

Lucas Mackie[1,*], Athanasios Angeloudis[2], Frederick Harcourt[1], Matthew D. Piggott[1]
[1]*Department of Earth Science and Engineering, Imperial College London, UK*
[2]*School of Engineering, Institute for Infrastructure & Environment, University of Edinburgh, UK*

*Summary:* The research presented here explores the potential to maximise income of a fleet of tidal lagoons when optimising adaptive control parameters to target peak prices in the Day-Ahead Energy Market. An adjustment algorithm is devised to represent the presence of lagoons in the price signal. Results indicate that the inherent phase difference present in the considered lagoon fleet serves to restrict a significant increase in price volatility, amplifying the benefits of income optimisation in comparison to the more traditional energy optimisation.

## Introduction

The recent rejection of a proposal to build and operate a tidal lagoon in Swansea Bay highlights the need to improve the value for money of such schemes for them to become a viable option in the UK energy mix. Research by Harcourt et. al. [1] explored the concept of using gradient-based optimisation techniques to exploit the predictability of tidal elevations and adaptability of hydraulic structure controls in tidal range schemes. Optimum control parameters are determined on a cycle-by-cycle basis to increase lagoon income by targeting times of high electricity price in the Day Ahead energy Market (DAM).

## Methods

Seven locations with pronounced tidal ranges along the west coast of England and Wales were selected for analysis. Consistency was kept with regards to lagoon design, including the implementation of an idealised circular impoundment of 40km$^2$. The lagoons also all operate bi-directionally with pumping intervals. Variability of turbine quantity was permitted to acknowledge discrepancies in tidal and bathymetric conditions. A 2D depth-averaged hyrodynamic model of the Irish Sea without lagoons was built using *qmesh, Thetis* and *Firedrake.* It utilised eight tidal constituents and provided site-specific tidal signals from which 0D models could simulate lagoon operation and calculate generated electricity. 2D modelling was used in favour of a harmonic analysis due to its capability to accurately represent areas of high tidal range, intertidal regions and tidal resonance effects. Validation of the resulting tidal signals was carried out by comparing model output with historic tide gauge data. Details of 2D and 0D models created using the same framework can be found in [2].

Lagoon income was calculated under two scenarios, both of which assume a perfect forecast of the obtained historic data. In the first, the original hourly price signal (OP) from Nord Pool is utilised [3]. The second applies an adjustment to this price signal (PA). This adjustment is proportional to the ratio between total energy generated by the lagoon fleet when using pre-determined optimum fixed control parameters and total energy traded in the DAM before the addition of the lagoons, the data for which is also provided by Nord Pool [3]. This is shown by:

$$p_{h,adj} = p_h \frac{E_{h,lf} + E_{h,m}}{E_{h,m}} \tag{1}$$

where, in a given hour, $p_h$ is the original price, $p_{h,\,adj}$ is the adjusted price, $E_{h,lf}$ is the energy generated by the lagoon fleet under a fixed control conditions and $E_{h,m}$ is the energy traded in the DAM.

An optimisation framework adapted from research by Harcourt et. al. [1] allows comparison of the lagoon fleet under different scenarios. Control parameters in the ebb and flood phase can be adapted with each cycle and make up a vector in a limited memory Broyden-Fletcher-Goldfarb-Shanno optimisation with limits. Three alternative optimisation files were created, which provided control parameters from which lagoons could be simulated over a year and have their energy output and income calculated. The first optimisation output imposed control parameters defined to an objective functional to maximise energy output (EM). This was then used to simulate lagoon operation using both OP and PA. The remaining two optimisation files established controls to a maximum income functional (IM), one using OP and the other with PA. All functionals adopted a two-cycle approach, where the controls in the first cycle are allowed to adapt but are fixed to pre-determined values in the second cycle. The

* Corresponding author.
*Email address*: l.mackie18@imperial.ac.uk

second cycle iteratively becomes the first in the subsequent round of optimisation and thus the optimisation steps forward in time. The consideration of the second tidal cycle has been accommodated to avoid the convergence to a sub-optimum water level in the following cycle on account of a short-sighted functional in the optimisation.

## Results

Table 1 summarises the generated income of the lagoon fleet under four simulations which utilise combinations of the two optimisation functionals and price signals. Results indicate an increase in income gain to the IM case once PA is applied. This can be attributed to the inherent phase difference present in the lagoon fleet. As can be seen by the inner water elevation profiles of the fleet in Fig. 1, lagoons in Swansea, Cardiff and Watchet, located in the Bristol Channel (BC), are out of phase from Colwyn, Liverpool, Blackpool and Solway, i.e. the lagoons north of Wales in the Irish Sea (IS), by about four hours. Due to the consistent operation of the fixed cycle control parameters, this phase difference is translated into the price signal adjustment. As a result, periods of generation will alternate between the two lagoon groups, and often occur while the other group expends energy to pump. The manifestation of this can be seen in Fig. 2 which shows the change in hourly price when BC and IS lagoons are applied separately. The line which represents the presence of all lagoons is often not far below and sometimes even higher in price than when just one of the two lagoon groups is applied. This suggests that the inherent phase difference serves to restrict the magnification of price signal volatility. By forecasting this effect, lagoons are therefore able to alter their control parameters to target peaks in electricity price, without risk of significantly reducing it. This serves to then amplify the benefits present when optimising control parameters to maximise income.

## Conclusions

The advantages of optimising a fleet of tidal lagoons to maximise income are magnified when the fleet can be subdivided into two groups which experience a significant phase difference in their operation. It permits the two groups to alternate generation and pumping periods, and therefore limit the impact that the presence of the lagoon fleet will have on the price of electricity in the DAM. Further work will seek to couple the 0D model with a 2D or 3D model to represent hydrodynamic interactions, update the price signal adjustment algorithm to reflect actual generation as opposed to idealised fixed control operation, and also implement a cost model component to further optimise individual schemes in the fleet.

*References:*

[1] Harcourt, F., Angeloudis, A., Piggott, M. D. (2019) Utilising the flexible generation potential of tidal range power plants to optimise econmic value. *Applied Energy.* **237**, 873-884

[2] Angeloudis, A., Kramer, S. C., Avdis, A., Piggott, M. D. (2018) Optimising tidal range power plant operation. *Applied Energy*. **212,** 680-690

[3] Nord Pool (2017) Historical Market Data. [Online]. Available: https:/www.nordpoolgroup.com/historical-market-data/

Table 1. Income of lagoon fleet under different optimisations.

| | Income (£) | | |
|---|---|---|---|
| Simulation | OP | PA | % diff. |
| EM | 844,922,063 | 718,375,395 | -14.98% |
| IM | 881,051,539 | 769,335,935 | -12.68% |
| % diff. | 4.28% | 7.09% | |

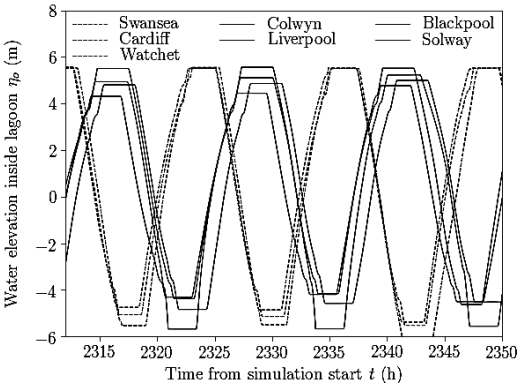


Fig. 1. Inner water levels of seven lagoons.

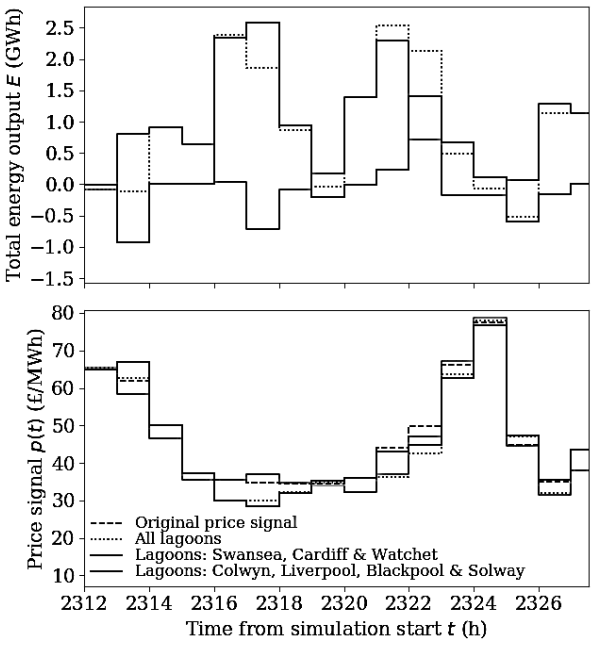


Fig. 2. Price signal and energy output of fixed control simulation.

# How bathymetric features affect turbine performance: Insights from a CFD model

Merel C. Verbeek*, Robert Jan Labeur
*Faculty of Civil Engineering and Geoscience, Delft University of Technology, NL*
Arnout C. Bijlsma, Tom S. D. O'Mahoney
*Deltares, NL*

*Summary:* In the presentation we discuss how flow separation downstream of irregular bathymetric features affects the theoretical power that can be extracted from a barrier, using results from a Computational Fluid Dynamics (CFD) model of the full scale tidal turbines which are installed in a Dutch storm surge barrier. Possibly, more power can be extracted from the considered channel geometry than estimated using depth-integrated models, as the turbines affected the flow separation downstream of a submarine sill, and hence the energy lost in turbulence dissipation.

## Introduction

Power output estimates of a farm or array of tidal stream turbines are often based on depth-integrated models. However, these models cannot predict the power available to energy harvesting at irregular bathymetric features where flow separation occurs in the vertical plane [1]. Possibly, the maximal power of channel geometries where flow separation occurs is higher than is estimated from depth-mean analyses, as the turbines deform the vertical velocity profile at irregular bed features, affecting the separating flow. This may reduce the kinetic energy lost in turbulence dissipation.

In this presentation we discuss how flow separation downstream of irregular bathymetric features affects the theoretical power that can be extracted from a barrier, using results from a Computational Fluid Dynamics (CFD) model of turbines which are installed in a Dutch storm surge barrier. The full-scale turbines are deployed close to an abrupt bathymetric feature, namely the sill of the barrier gate. The flow separates downstream of the sill and energy is dissipated in a turbulent eddying motion in a large recirculation zone.

## Methods

The influence of an abrupt step in the bed, a sill of the storm surge barrier, on the hydrodynamics and the production of the turbines can be investigated for a situation with a turbine array upstream of a sill (ebb) and one for a situation with turbines downstream of a sill (flood). For this purpose, A 3D Volume of Fluid CFD model of the flow past a gate with turbines plus two half gates on either side was developed in previous work using the Star-CCM software [2], [3]. An array of five turbines is modelled in the centre gate, using a local rotating mesh and Eddy Simulation. The model has been validated using data from a field monitoring campaign [3]. In this presentation, four stationary model runs are considered: two for a head loss of 0.55 m (flood situation) and two for a head loss of 0.32 m (ebb situation), both for a situation with - and without turbines. Although the modelling was done for smaller head differences during the ebb phase than during the flood phase, a preliminary comparison between these situations is made in this presentation based on the flow phenomenology.

## Results

The model provides insight in the spatial distribution of the flow over the domain for a situation with turbines upstream and downstream of a sill. While the discharge through the domain was nearly the same when the turbines were downstream of the sill for all considered cases (flood), the discharge decreased noticeably with respect to the reference situation without turbines when the turbines were upstream of the sill (ebb) (Fig 1b). In the first situation, the flow velocity below the turbines, the so-called turbine-scale bypass, increased and the recirculation zone downstream of the sill is reduced in depth and length (Fig 1c-right). This was not observed for the simulation with turbines upstream of the sill (Fig 1c-left). Besides, the calculated energy production of the turbines in the model is higher when the turbines were situated downstream of the sill (flood) than when they were upstream of the sill (ebb), when accounting for the difference in head loss. This is in line with previous work [4], and can be explained by the larger mass flux through the rotors in the situation with turbines downstream of the sill.

* Corresponding author.
*Email address*: m.c.verbeek@tudelft.nl

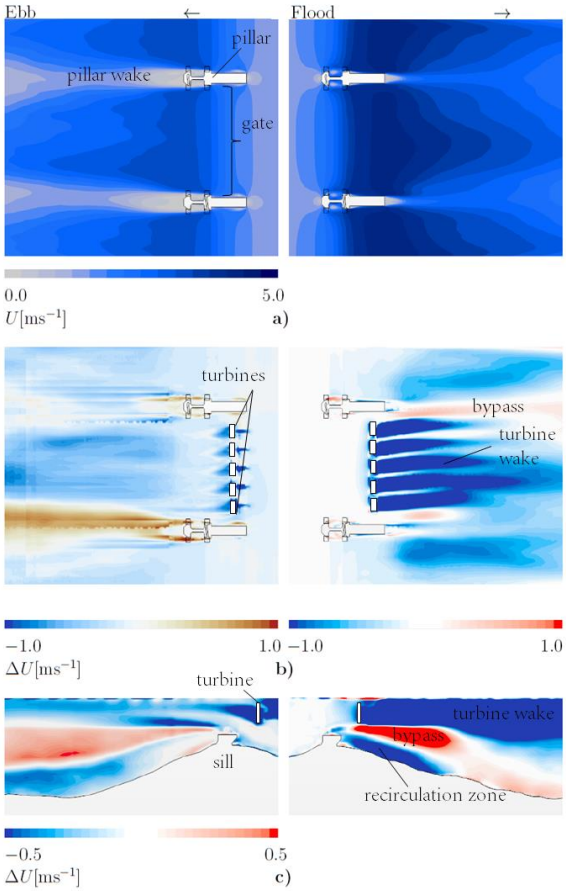


Fig. 1.
a) The reference situation without turbines: The modelled time-averaged flow field in one gate and two half gates of the storm surge barrier in a horizontal cross-section at -5 m NAP (national reference datum) (left: ebb situation with flow to the left, right: flood situation with flow to the right). The gates consist of pillars and a bottom sill.
b) The modelled time-averaged flow field for a situation with turbines minus the situation without turbines in one gate and two half gates of the storm surge barrier in a horizontal cross-section at -5 m NAP (at turbine-axis height). The five turbines positions are indicated with white boxes. (The asymmetry in the bypass downstream of the pillars is possibly a consequence of the asymmetric bed topography downstream of the gate.)
c) The modelled time-averaged flow field for a situation with turbines minus the situation without turbines in a vertical plane at the location of the axis of 4th turbine of the array (counting from the top). The bypass velocity is much larger in the flood situation, resulting in a smaller recirculation zone

## Discussion and conclusion

The orientation of the turbines with respect to the sill can possibly be optimized to harvest more energy from the flow. The power output is a function of – among other things – the discharge through the channel, hence understanding how the discharge responses to the added resistance of the turbines is important. As expected, the discharge through the flow domain reduced noticeably when turbines were added upstream of the sill. However, the discharge remained nearly the same, when the turbines were added downstream of the sill. The following physics may play a role in this observation. The turbines – when located downstream of the sill - decreased the shear in the vertical flow velocity profile downstream of the sill. Consequently, the size of the recirculation zone downstream of the sill and its velocities were much smaller. The turbines may have reduced, in this way, the energy lost in the flow separation.

This may imply that for power estimates for tidal turbines near or at pronounced bathymetric features the configuration of turbines with respect to bathymetric features should be considered. Possibly, more energy can be extracted from the considered channel than is expected from depth-integrated modelling, as the turbines can affect flow separation processes and hence the kinetic energy lost in turbulence dissipation at these locations.

*Acknowledgements:*

This work is part of research programme The New Delta (869.15.008), which is financed by the Netherlands Organization for Scientific Research (NWO). The European Regional Development Fund (ERDF) OP-Zuid 2014-2020 programme is acknowledged for their support.

*References:*

[1] Adcock, T. A., Draper, S., Nishino, T., Tidal power generation – a review of hydrodynamic modelling. Proc. Inst. Mech. Engrs A 0, 1–17, 2015
[2] Tralli, A. Bijlsma, A., te Velde, W., de Haas, P. CFD study on free-surface effect influence on tidal turbines in hydraulic structures, Proceedings of the ASME 2015, 34th OMAE, 2015, p. 41187.
[3] O'Mahoney, T. S. D., de Fockert, A, Bijlsma, A.C., de Haas, P, Hydrodynamic impact and power production of tidal turbines in a storm surge barrier, 13th EWTEC, 2019 (submitted)
[4] Verbeek, M.C., Labeur, R.J., Uijttewaal, W.S.J., The performance of a weir-mounted tidal turbine: Field observations and theoretical modelling, 2019 (in prep.)

# Agent-based modelling of fish collisions with tidal turbines

K Rossington*, T Benson
*HR Wallingford Ltd, Wallingford, Oxfordshire, UK*

*Summary:* Interest in marine tidal turbines, particularly in coastal waters, raises concerns about collisions between marine wildlife and underwater turbine blades. Existing collision risk models are based on analytical solutions which assume simplistic non-behavioural traits. Here we extend an existing numerical Agent-Based Model (ABM) to model collisions and represent realistic behaviours of marine species. The new ABM successfully reproduces collision rates as predicted by the analytical Collision Risk Model (CRM) (Band et al., 2016) [1] showing that both approaches are equivalent.

## Introduction

With increasing developments in marine renewable energy, coupled with high densities of marine species in suitable installation locations, there is concern that fish and marine mammals could collide with underwater devices resulting in injury or fatality. This paper describes the development of a collision model coupled with a Lagrangian ABM of fish swimming behaviour in a simulated hydrodynamic environment to predict collisions with underwater devices. Collision estimates for the developed model were compared with predictions from the original CRM of Band et al. (2016)[1].

## Model description

*HydroBoids* is an agent-based model (ABM) for predicting the movement of fish (or other mobile marine animals) and consequences of behaviours in response to stimuli such as sound, water properties or chemical tracers [2,3]. In the model, individuals are represented as Lagrangian points in a three dimensional underwater space which are advected by the Eulerian hydrodynamic flows calculated using the TELEMAC modelling system (www.opentelemac.org).

Each fish is assigned characteristics or traits that are both *physiological* (e.g. swim speed) and *behavioural* (e.g. schooling). The physiological characteristics of the fish are assigned across the population from a normal distribution to account for natural variability. Fish swim using a correlated random walk and may follow environmental gradients, such as salinity. Fish behaviours are based on the current state of the fish, which leads to a probability of certain behaviours occurring. These are compared with a randomly generated number to determine which behaviours occur on any time step.

Underwater turbines ('rotors') occupy a three-dimensional space within the underwater environment described by the model domain. The impact of the rotors on the flow is not included. On each time step, the checks are made as to whether any fish have passed through the space occupied by the rotor (termed a *transit*). For each transit, the probability of collision is calculated using the equation described by Band et al. (2012) [4]:

$$p(r) = \frac{b\Omega}{2\pi v}\left(|\pm c\ sin\ y + \alpha\ cos\ y| + max\{L, W\alpha\}\right) \quad (1)$$

where *p(r)* is the probability of collision as a function of radius, *b* is the number of blades in the rotor, $\Omega$ is the angular velocity, *c* and $\gamma$ are the chord and pitch of the blade at radius *r*, *v* is the velocity of the marine animal, *L* is body length of the animal, *W* the animal's width and $\alpha = v/r\Omega$.

Whether or not a transiting individual collides with the rotor is then determined stochastically by comparing the probability of collision for each transit against a randomly generated number between 0 and 1 – if the probability of collision exceeds the random number, a collision has taken place (Figure 1).

## Results

The ABM was used to simulate fish swimming through a turbine in different conditions, including transit direction, transit speed and for different fish body lengths. Fish transiting in an upstream direction were more likely to collide than those swimming downstream (with the flow) due to the shape of the turbine blades. Slower swimmers and longer body lengths were also predicted to have increased collision rates. Average collision rates from the ABM were comparable with collision probabilities predicted using the CRM [1,5] (Table 1). Collisions were assumed fatal for closing velocities exceeding 5 m/s; typically 10-15% of collisions in this test case.

* Corresponding author.
*Email address*: author@affiliation.ac.uk

Table 1 Comparison of average collision rates predicted using the ABM and the collision probability from the CRM (SNH, 2016) [5].

| Scenario | Initial direction | Travel velocity of fish (*v*) (m/s) | Body length (m) | Average collision rate (*ABM*)* | Collision Probability (CRM) |
|---|---|---|---|---|---|
| 1 | Downstream | 1.5 | 0.5 | 16% | 16% |
| | Upstream | 1.5 | 0.5 | 23% | 23% |
| 2 | Downstream | 1 | 0.5 | 20% | 20% |
| | Downstream | 1.5 | 0.5 | 16% | 16% |
| | Downstream | 2 | 0.5 | 15% | 15% |
| 3 | Downstream | 1.5 | 0.2 | 11% | 10% |
| | Downstream | 1.5 | 0.5 | 16% | 16% |
| | Downstream | 1.5 | 0.8 | 22% | 22% |

** predicted number of collisions divided by the total number of transits, averaged over five simulations.*

## Conclusions

The ABM produced collision rates comparable to the CRM in benchmark tests. It has advantages over traditional collision risk models because the animal density in the region does not need to be known *a priori*, but instead is calculated by the ABM dependent on the behaviours assigned to the individuals. The inclusion of different swimming behaviours in the ABM changes the predicted collision rate [3]. The modelling approach also opens up the potential to simulate avoidance and attraction behaviours.

*References:*

[1] Band, B., Sparling, C., Thompson, D., Onoufriou, J., San Martin, E., & West, N. (2016). Refining Estimates of Collision Risk for Harbour Seals and Tidal Turbines (Vol. 7). https://doi.org/10.7489/1786-1

[2] Rossington, K., Benson, T., Lepper, P. & Jones, D. (2013). Eco-hydro-acoustic modelling and its use as an EIA tool. *Marine Pollution Bulletin*, **75**, 235-243.

[3] Rossington, K., & Benson, T. (submitted). An Agent-Based Model to predict fish collisions with tidal stream turbines.

[4] Band, B. (2012). Using a collision risk model to assess bird collision risks for offshore windfarms, 2(March), 62. https://www.bto.org/sites/default/files/u28/downloads/Projects/Final_Report_SOSS02_Band1ModelGuidance.pdf

[5] Scottish Natural Heritage. (2016). Assessing collision risk between underwater turbines and marine wildlife. SNH guidance note.

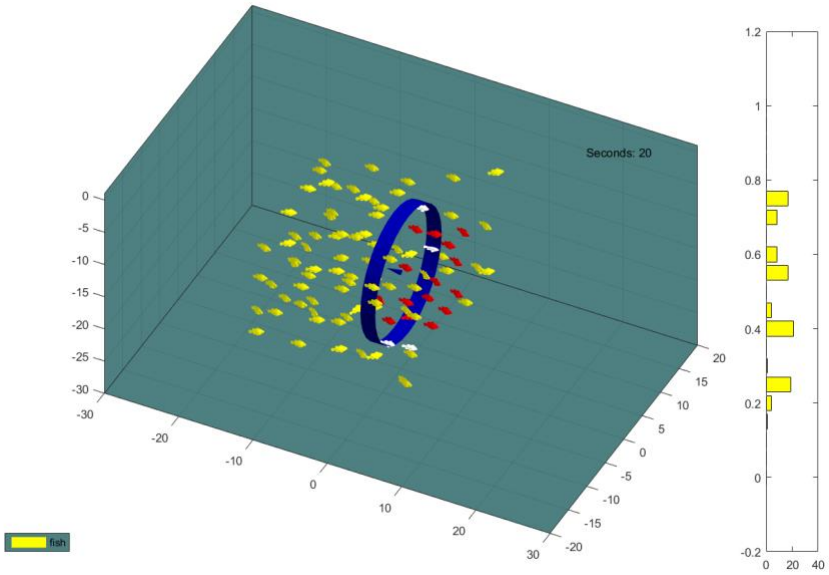


Figure 1 Modelled fish swimming through a turbine (Yellow fish have not collided, red have collided but were not killed and white fish were killed by a collision).

# Empirical orthogonal functions for decoupling waves and turbulence in ADCP measurements

Michael Togneri*, Ian Masters, Iain Fairley
*Marine Energy Research Group, College of Engineering, Swansea University, UK*

*Summary:* ADCP estimates of turbulent kinetic energy (TKE) are usually obtained with the variance method. A shortcoming of this method is that any significant wave action will contaminate the estimate. We use a month-long ADCP dataset to examine the effectiveness of empirical orthogonal function (EOF) analysis to separate the contributions of turbulence and waves to the ADCP estimate of TKE. The effectiveness of the separation is tested by comparison with linear theory. We demonstrate the wave-turbulence decoupling on the case study and discuss its advantages and disadvantages.

## Introduction

The variance method uses a weighted sum of beam variances from each of the beams of an ADCP to estimate TKE, which measures the energy contained in turbulent velocity fluctuations per kilogram of fluid [1]. With this technique any source of variance other than the turbulence will also contribute to the estimate – most significantly, the variance associated with orbital wave motions. Thus, this estimate of TKE is biased high by wave action, sometimes by so much that the estimate is high by an order of magnitude [1].

For datasets that are at least intermittently wave-dominant, waves will likely be associated with a statistically significant data mode. EOF analysis should then pick out statistical modes that approximate the physical mode due to wave action. We perform such an analysis on a previously-examined ADCP dataset, supplemented by simultaneous measurements from a wave buoy giving us an independent measure of wave properties – we use this data to calculate parameters for a linear theory analysis of the waves to compare with the EOF analysis.

## Methods

A two-month ADCP dataset from off the coast of Anglesey is analysed. This dataset was collected between 9-11/14, and consists of 15-minute bursts of data collected at 2Hz every hour throughout the deployment – this sampling frequency is sufficiently high to capture all significant energy-bearing fluctuations. In addition, a wave buoy ca. 2km from the ADCP measured wave direction, significant wave height and observed wave period. The variance method is used to estimate TKE $k$ from the ADCP measurements as standard, but to account for the putative effects of wave contamination, we call the estimate $k_{ADCP}$ and assume it can be simply decomposed into wave and turbulent contributions as $k_{ADCP} = k_t + k_w$.

We demonstrate that, following Airy wave theory, there is a simple analytical expression for the expected form of $k_w$ and that all the necessary information to fully specify this form can be obtained from the wave buoy.

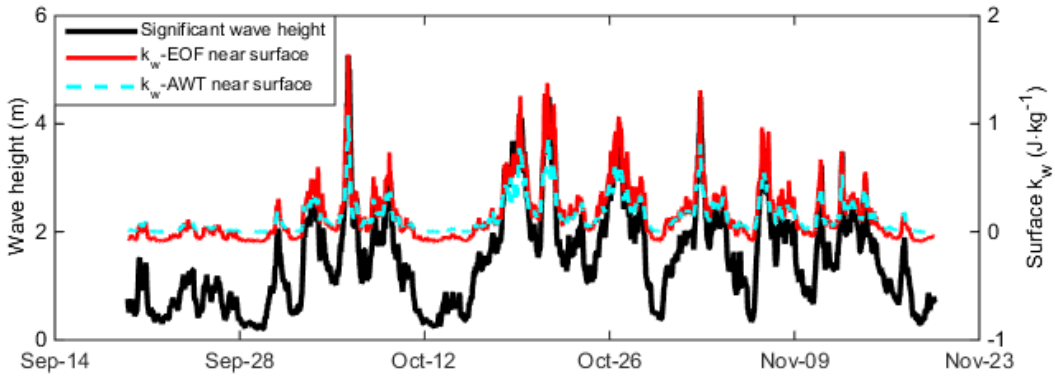


Fig. 1: Comparison of (left axis) significant wave height as measured from buoy with (right axis) near-surface wave pseudo-TKE estimated using EOF analysis ($k_w$-EOF) based on ADCP measurements, and Airy wave theory ($k_w$-AWT) based on wave buoy measurements.

* Corresponding author.
*Email address*: M.Togneri@swanesa.ac.uk

A standard EOF analysis is performed on the $k_{ADCP}$ dataset, and we assume that the first EOF represents the contribution of wave action. This captures only the wave-related variability in $k_{ADCP}$, but omits any mean bias. To estimate this bias, we take a weighted mean of all the data at times of negligible wave action to be a "turbulence-only" mean, with the remainder of the mean due to wave action. Combining this mean value with the first EOF of $k_{ADCP}$ yields a second estimate of $k_w$, fully independent from the Airy theory estimate.

## Results

We see in figure 1 that the two estimates of $k_w$ are very similar to one another across the whole dataset, and that they are closely associated with wave action. All three parameters plotted here are very highly correlated with one another, such that $R = 0.94 - 0.96$ for any two of the three. This gives us confidence that the statistical mode captured by EOF analysis does have an approximate correspondence to the physical wave contribution.

Based on this, we carry out a wave-turbulence decoupling as shown in figure 2. This appears to be very successful, in that there is very little obvious trace of wave action remaining in the estimate of $k_t$, and $k_w$ is negligibly small at times of low wave heights.

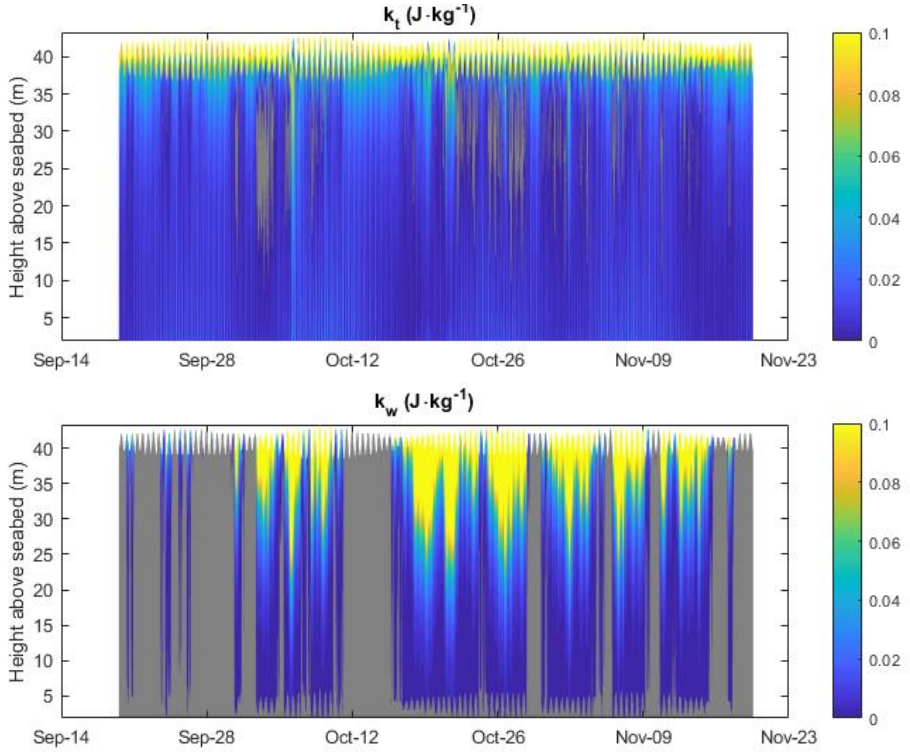


Fig. 2: Separation of $k_{ADCP}$ into turbulent ($k_t$) and wave ($k_w$) contributions. Values below zero are shown in grey.

## Conclusions

We have shown that it is possible in principle to remove wave contamination from an ADCP estimate of TKE without any supplementary data. Our estimate of the wave contribution agrees reasonably well with predictions from linear theory. ADCPs with a vertical beam devoted to surface-tracking could in theory replicate the role of the wave buoy data in the current study, giving two independent methods of wave-turbulence decoupling from a single device.

*Acknowledgements:*

The authors acknowledge the support of ERDF through the Atlantic Area project MONITOR (EAPA_333/2016). The data were collected as part of the ERDF projects SEACAMS and SEACAMS2.

*References:*

[1] M. T. Stacey, S. G. Monismith and J. R. Burau, "Measurements of Reynolds stress profiles in unstratified tidal flow," *J. Geophys. Res.*, vol. 104, pp. 10933-10949, 1999

[2] M. Togneri, M. Lewis, S. Neill and I. Masters, "Comparison of ADCP observations and 3D model simulations of turbulence at a tidal energy site," *Renew. Energ.*, vol. 114, pp. 273-282, 2017

# Characterising the FloWave Facility with a Steady State CFD Model

Matt Edmunds[1], Alison J. Williams, Ian Masters.
*College of Engineering, Swansea University, UK*

*Summary:* This work demonstrates an attempt to characterisation of the FloWave facility using a steady state computational fluid dynamics (CFD) model. This work is undertaken to establish a baseline for model validations such as blade element momentum CFD (BEM-CFD). The results show a reasonable correlation to measured data obtained from FloWave and highlights some of the assymetric characteristics of the turbulence.

## Introduction

Simulating tidal turbines is computationally expensive when utilising computational fluid dynamics (CFD) models. The advantages of using CFD is the ability to predict the downstream interacting wakes. With this in mind, the use of a steady state model, such as BEM-CFD [1], would be of great benefit to the industry. To validate such a model, thus providing confidence in its use, can be achieved by first comparing to laboratory scale experiments [2]. Once this is complete, a more robust validation of the model in a more extreme environment would be important i.e. FloWave [3]. The first step in this process is to characterise the facility to obtain a baseline model to which devices can be installed and thus validated. However, unlike a simple flume, the characteristics of FloWave are tricky to capture using only a steady state simplified model of the domain.

## Results

Figure 1 demonstrates the general distribution of flow across to tank. The inlet flow is directed downstream from the inlet vents, accelerating towards the centre of the tank. A fairly uniform distribution of flow is observed at the centre of the tank. Figure 2 show velocity and turbulence intensity plotted along the centreline of the tank at a height of 1 metre. The simulated results are over plotted showing good agreement with measured results. Figure 3 shows velocity and turbulence intensity plotting along the y-axis at the centre of the tank, also demonstrating good correlation at this location. However, it is noted that there is an asymetry to the turbulence at this location which appears to increase downstream (see Figure 4).

## Conclusions

It is possible to simulate a complex flow regime using steady state CFD solvers. The results demonstrate good agreement with experiment. The exception here is the assymetric nature of the tubulence generated within the tank. It was not necessary to model the tank in its entirety i.e. from inlet to outlet vents only. This reduced the complexity significantly. This work demonstrates that the use of this type of model for the robust validation of BEM-CFD models, is achievable.

*Acknowledgements:*
The work was also supported by the EPSRC funded "Extension of UKCMER Core Research, Industry and International Engagement" project (EP/M014738/1). The Author(s) acknowledge(s) the financial support provided by the Welsh Government and Higher Education Funding Council for Wales through the Sêr Cymru National Research Network for Low Carbon, Energy and Environment. (C001822).

*References:*

[1] M. Edmunds, Alison J. Williams, I. Masters, and T. N. Croft. An enhanced disk averaged CFD model for the simulation of horizontal axis tidal turbines. *Renewable Energy*, 101:67 – 81, 2017.

[2] Paul Mycek, Benoît Gaurier, Grégory Germain, Grégory Pinon, and Elie Rivoalen. Experimental study of the turbulence intensity effects on marine current turbines behaviour. Part I: One single turbine. *Renewable Energy*, 66(0):729 – 746, 2014.

[3] University of Edinburgh. FloWave Ocean Energy Research Facility. https://www.flowavett.co.uk/, 2018. Retrieved: May 2018.

[1]Corresponding author.
*Email address:* m.edmunds@swansea.ac.uk

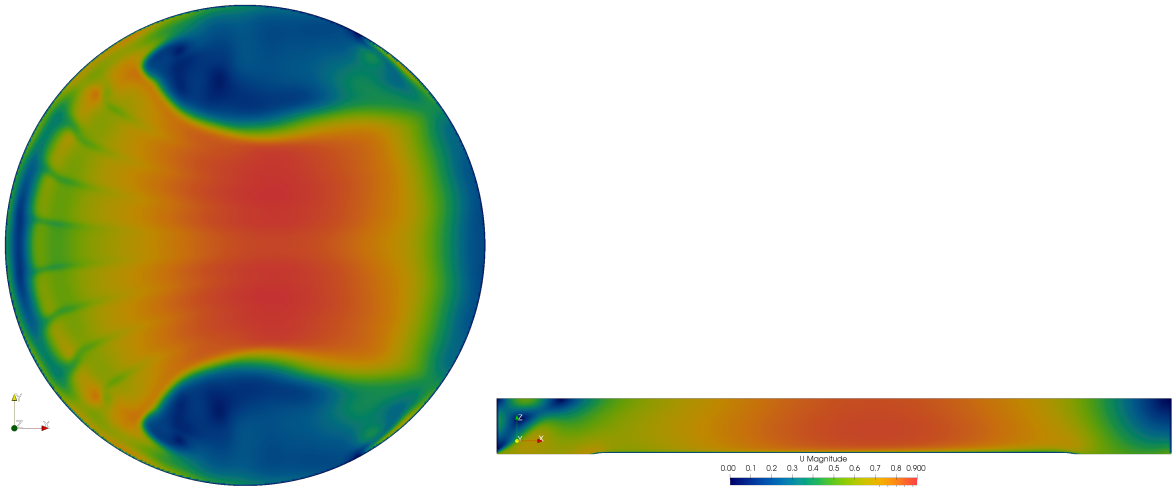


Figure 1: The left image is a slice taken at 1m depth on the x-y plane and the right image shows a virtical slice on the x-z plane through the centre of the tank. Colour is mapped to velocity in m/s.

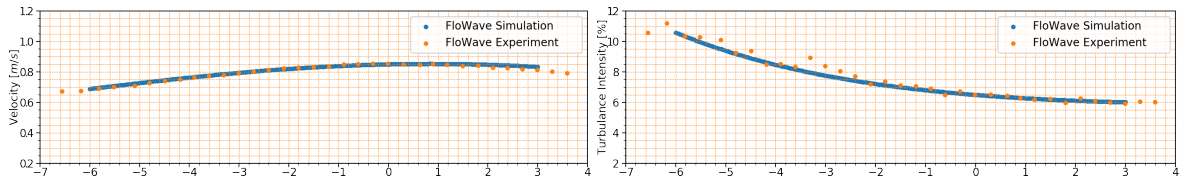


Figure 2: The left image is a graph of velocity plotted against x-axis location along the centre of the tank at a height of 1 metre, and the right image is a graph of turbulence intensity along the same axis.

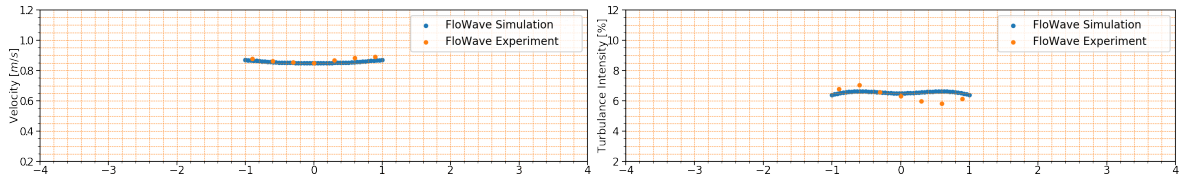


Figure 3: The left image is a graph of velocity plotted against y-axis location along the centre of the tank at a height of 1 metre, and the right image is a graph of turbulence intensity plotted against y-axis at the same location.

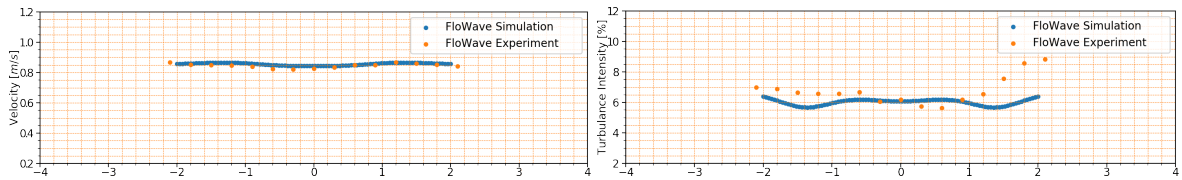


Figure 4: The left image is a graph of velocity plotted against y-axis location set at 2.4 metres downstream of the tank centre at a height of 1 metre, and the right image is a graph of turbulence intensity plotted against y-axis at the same location.

# Experimental study on interactions between two closely spaced rotors

James McNaughton[1], Bowen Cao, Christopher Vogel, Richard H. J. Willden
*Department of Engineering Science, University of Oxford, UK*

*Summary:* The tidal turbine industry does not currently account for blockage in rotor design, meaning that potential impacts on turbine thrust and power are not yet realised, nor fully understood. Following prior theoretical [1] and numerical [2] work to quantify performance benefits, a rotor has been designed and tested to better-understand potential performance benefits and flow physics associated to closely spaced tidal turbine rotors. Preliminary results show that moving from a single to twin configuration a 20% increase in power is achievable for a 10% increase in thrust at the nominal design point.

## Introduction

That a turbine's performance can increase when deployed in a blocked flow is not significant in itself. However, Schluntz and Willden [3] demonstrated that by incorporating blockage in the design process the benefits can be exploited further. More recently, Vogel & Willden [2] simulated a fence of four tidal turbines with a tip-to-tip spacing of 1d (diameter), demonstrating the variability of thrust and power across the fence due to different rotor designs and control strategies. A multi-rotor fence concept is being developed with the turbines designed to exploit the constructive interference effects arising from high local ($B_L$) yet low global ($B_G$) blockage, defined by:

$$B_L = \frac{\pi\, d^2/4}{h(s+d)}, B_G = \frac{n\pi\, d^2/4}{hw}$$

See Fig. 1 for defining dimensions. This work presents initial results of power, thrust and flow measurements associated to a single turbine's performance change when a second rotor is positioned next to it.

## Methods

A 1.2 m rotor was designed using a Reynolds-Averaged Navier-Stokes embedded Blade Element design tool to account for the higher blockage conditions (further details in [4]) with blades and hub components CNC'd from aluminium. The rotors were designed to mate to the University of Edinburgh's turbine nacelles, described in [5]. Two configurations were tested: a single turbine and two side-by-side rotors (Fig. 2) with a close tip-to-tip spacing ($s = d/4$) which gave a local blockage of 37%.

Turbine performance was measured using a torque and thrust transducer, whilst blade root bending moments were measured in flap and edgewise directions. Flow was measured at hub-height in a variety of locations using an ADV, with the upstream reference velocity measured 2d upstream of the single rotor. Performance curves of power and thrust coefficients were obtained over a range of tip-speed ratios (TSRs). For this work, 5 minute averaged data is used to discuss mean values only.

## Results

The power coefficients for the same turbine in the single and twin configurations are shown in Figure 3. Here the values have been normalised by the power coefficient of the single turbine at the nominal TSR so that variations can be easily identified. At the nominal TSR a 20% increase is observed in the power coefficient, which results from a 10% increase in thrust (Figure 4). Addition of the second rotor also indicates that the design TSR for maximising power increases marginally as suggested by theory and computation.

## Conclusions

Initial analysis of averaged quantities shows that a substantial increase in power can be achieved by designing for and then placing a second rotor in close side-by-side proximity. Further analysis will be performed to understand unsteady interactions between the two rotors using measured flap and edgewise root bending moments, and how performance benefits change when the rotors are controlled at different TSRs.

[1] Corresponding author.
*Email address*: james.mcnaughton@eng.ox.ac.uk

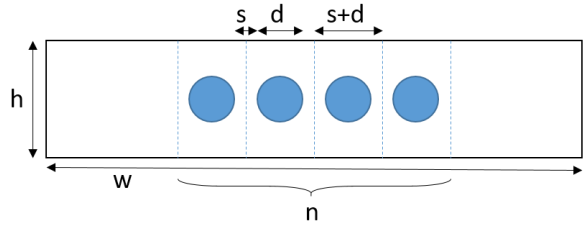


Fig 1. Diagram showing dimensions used to define local and global blockage (not to scale).

Fig 2. Photo of the turbines operating during the tests.

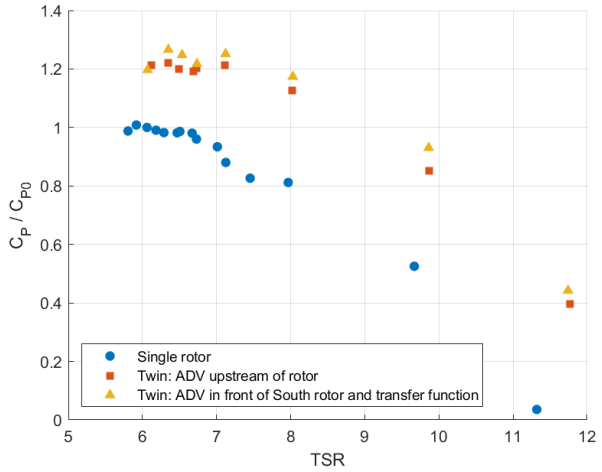


Fig 3. Power coefficient for single and twin configurations. All $C_P$ values are normalised by the single turbine's power coefficient at nominal TSR.

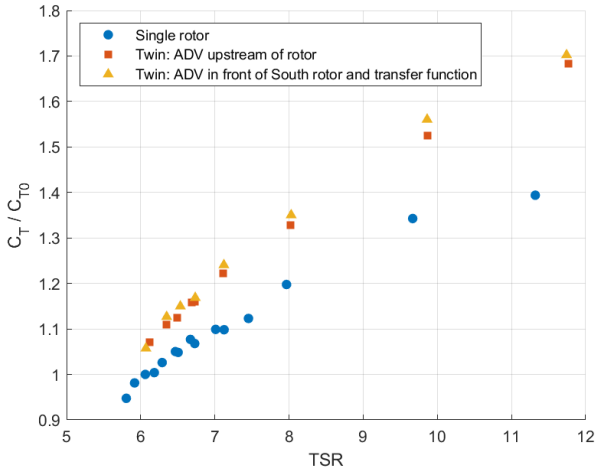


Fig 4. Thrust coefficient for single and twin configurations. All $C_T$ values are normalised by the single turbine's thrust coefficient at nominal TSR.

*Acknowledgements:*

The authors would like to thank: SuperGen Marine, Wave Energy Scotland and EPSRC (grant no.'s EP/R007322/1 and EP/R007322/1) for supporting the research; SIMEC Atlantis Energy for useful comments and discussions; Gregory Payne, Tim Stallard and Jeff Steynor for guidance in rotor design; Tom Davey, Anup Nambiar and Edd Nixon for their support prior to and throughout the tests; the University of Edinburgh for loaning two of their nacelles for use in the project; Steven Ettema, Federico Zilic de Arcos and Daniela Taira for their contributions to the testing.

*References:*

[1] Nishino, T. and Willden, R. H. J. (2013). Two-scale dynamics of flow past a partial cross-stream array of tidal turbines. *Journal of Fluid Mechanics*, **730**, 220–244.

[2] Vogel, C. R. and Willden, R. H. J. (2017). Multi-rotor tidal stream turbine fence performance and operation. *International Journal of Marine Energy*, **19**, 198–206.

[3] Schluntz, J. and Willden, R. H. J. (2015). The effect of blockage on tidal turbine rotor design and performance. *Renewable Energy*, **81**, 432–441.

[4] Cao, B., Willden, R. H. J. and Vogel, C. R. (2018). Effects of blockage and freestream turbulence intensity on tidal rotor design and performance. In: *3rd International Conference on Renewable Energies Offshore*.

[5] Payne, G. S. Stallard, T. Martinez, R. and Bruce, T. (2018). Variation of loads on a three-bladed horizontal axis tidal turbine with frequency and blade position. *Journal of Fluids and Structures*, **83**, 156–170.

# Hydrodynamics, PTO and control design of a horizontal-axis model turbine for experimental research

Z. Sarichloo[1], M. Rafiei[1,2], F. Giulii Capponi[2], F. Salvatore[1*]
[1]*CNR-INM, Consiglio Nazionale delle Ricerche, Istituto di Ingegneria del Mare, Rome, Italy*
[2]*Università degli Studi di Roma "La Sapienza", Rome, Italy*

*Summary:* The development of a model horizontal-axis turbine for research on tidal energy conversion mechanisms at the Institute of Marine Engineering of the Italian National Research Council (CNR-INM, former INSEAN) is presented. Approaches used for the rotor hydrodynamic design and for the definition of the PTO system and power control strategies are described and preliminary results from ongoing work are discussed.

## Introduction

Experimental studies of small scale hydrokinetic turbines in towing and flume tanks provide fundamental knowledge on tidal energy conversion mechanisms. They also represent a necessary stage in the development of converters technology and provide benchmark data for the validation of CFD and computational tools for design.

CNR-INM is carrying out the design and realization of a laboratory-scale model horizontal-axis turbine for multi-disciplinary research. The objective is to perform a wide range of experimental activities on turbine blade and wake hydrodynamics as well as to analyse power control strategies when the turbine operates in transient flow conditions describing real operation in a tidal site. This includes the effects of onset flow turbulence and large scale eddies, as well as the effects of wave/current interactions for single devices and for arrays.

## Methods

Considering the research nature of the present project, power output maximization is not a design objective, while requirements are imposed to adapt model turbine performance to limitations of the supposed testing facilities and equipment. In particular, rotor diameter of 0.65 m is found as an optimal value to limit blockage effects of a single device in the flume tank and of small arrays in the towing tanks at CNR-INM. Reference testing speed of 2-3 m/s is considered to operate at Reynolds number values adequate to describe conditions of larger scale models tested at sea. Considering testing speed, a relatively low design TSR of 3.5 has been identified to match limitations of thrust and torque measuring equipment.

The hydrodynamic design procedure is based on an original hybrid iterative approach combining blade element momentum theory valid for two-dimensional wind/tidal turbine flows and a Boundary Integral Equation Model with viscous-flow correction (BIEM-VFC) valid for three-dimensional flows around turbines in arbitrary onset flow. BIEM-VFC validation studies are presented in [1-2]. The methodology allows to correctly describe turbine performance over a range of operating conditions close to design, while at very low TSR the simple viscous-flow correction applied may result into inaccurate predictions of thrust and power.

A hydrofoil representing blade sections is chosen in order to have high lift-to-drag efficiency, while lift and drag properties over a Reynolds number range are determined using the X-Foil code. Given the design TSR, blade momentum theory provides optimal distributions of blade pitch and chord. These distributions do not account for three-dimensional flow effects induced by turbine wake as well as nacelle perturbation. However, these distributions are taken as initial guess for an iterative procedure in which turbine performance is predicted by BIEM-VFC. This provides an effective angle of attack correction to update blade pitch distribution and to match a target angle of attack distribution along blade span. Simple structural conditions are considered to determine sectional profile thickness and camber after parametrization of the reference hydrofoil shape.

The physical turbine model will be equipped with transducers to measure thrust and torque at rotor shaft, while a 6-DoF sensor in-house developed at CNR-INM will provide single blade loads. The rotor will be connected to a power train consisting of an electric generator and its power control system. The application of reliable control technologies for tidal stream turbines is still at an early stage of development as compared to mature technologies like wind energy. Many fundamental and applied issues are addressed in the literature that should be faced to significantly improve the efficiency, operation, and life-time of TSTs. The PTO system for marine turbines need to have a good efficiency, high reliability and long service life with reasonable maintenance requirements and low cost. Therefore, the direct-drive permanent magnet synchronous generator

* Corresponding author.
*Email address*: francesco.salvatore@cnr.it

(PMSG) and fixed blades without yaw system represents an appealing solution, which does not require variable pitch and yawing mechanisms, gearbox, and brushes [4]. These characteristics inspire the PTO and control system design considered in the present study. Special attention is given to the scalability of solutions relevant for full-scale devices into a small model sized for testing at laboratory scale in towing and flume tanks.

The proposed layout consists of a direct-drive PMSG decoupled from the electrical grid through a full-power converter, which consists of two voltage source converters (VSC) connected in a back-to-back configuration with an intermediate DC link capacitor (right Fig. 1). This topology is appropriate for bi-directional current flows and is compatible with developing a Maximum Power Point Tracking (MPPT) strategy for the system.

In particular, two types of control strategies, torque and speed control, for the generator-side converter of direct-drive PMSG, in steady and unsteady inflow conditions, are proposed. Mathematical models of the hydrodynamic conversion and PMSG are developed and implemented in Simulink. The hydrodynamic model by BIEM-VFC is used to determine a full series of turbine performance simulations in both steady and unsteady onset flow conditions. This provides a comprehensive characterization of the turbine loading spectrum over a relevant range of operational conditions. The main challenge for the control system is the fluctuation of TSR which is the result of unsteady onset flow and constrained RPM. The aim for the simulations is to evaluate performance of the proposed control strategies and to limit the harmonic problems because of the mentioned fluctuation as much as possible.

## Results

At present, the hydrodynamic and mechanical design of rotor and nacelle components is nearly completed. In parallel, the PTO system architecture and suitable control strategies are investigated through simulations. At the Workshop, the hydrodynamics and electrical/control design procedures will be described and preliminary results of the design procedure for a three-bladed axial turbine with D=0.65 m, design TSR=3.5 and Worthmann FX blade sections will be presented and discussed (left Fig. 1).

## Conclusions

The development of a model turbine for experimental research is underway at CNR-INM. An original procedure for the hydrodynamic design of blades has been proposed and applied to determine a rotor with imposed characteristics. The PTO unit is based on a direct-drive PMSG combined with torque and speed control system and a Simulink model has been implemented to determine optimal design parameters for a given range of operating conditions. The model turbine will be used for studies in flume and towing tanks aimed at reproducing at laboratory scale flow conditions relevant for real tidal sites.

*References:*

[1] Salvatore, F., Calcagni, D., Sarichloo, Z. “Development of a Viscous/Inviscid Hydrodynamics Model for Single Turbines and Arrays,” EWTEC 2017, Cork, Ireland, 2017.

[2] Salvatore, F., Sarichloo, Z., Calcagni, D., “Marine turbine hydrodynamics by a boundary element method with viscous-flow correction,” J. Marine Science and Eng., Vol. 6 (53), 2018.

[3] Sarichloo, Z., Salvatore, F., Di Felice, F., Costanzo, M., Starzmann, R., Frost, C., “Computational analysis and experimental verification of a Boundary Integral Equation Model for tidal turbines,” RENEW 2018 Conference, Lisbon, Portugal, October 2018.

[4] Rafiei, M. , Salvatore, F., Giulii Capponi, F. “Generator Topologies for Horizontal Axis Tidal Turbine,” in progress of ELECTRIMACS 2019, Salerno, Italy, May 2019.

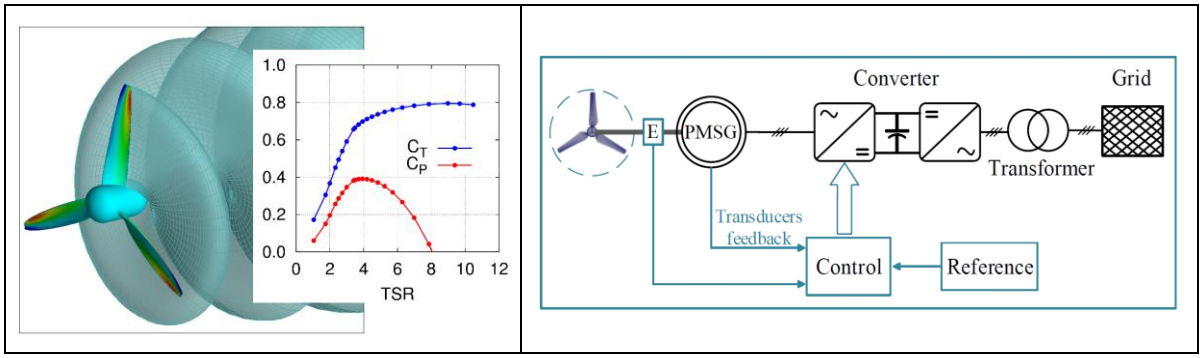


Fig. 1. Hydrodynamic modelling of the turbine using BIEM-VFC (left); PTO and control system layout (right).

# The Effects of Surge Motion on Floating Horizontal Axis Tidal Turbines

Mohamad H. B. Osman*, Richard H. J. Willden, Christopher Vogel
*Department of Engineering Science, University of Oxford, UK*

*Summary:* Wave induced motions due to actual sea state conditions will impact on the performance of floating horizontal axis tidal turbine systems. This paper presents the results from numerical simulations of a 3-bladed horizontal axis tidal turbine oscillating in surge motion in a moving reference frame. The turbine was simulated at its optimum tip-speed ratio, $\lambda$ = 4.4, using the *k-ω SST* turbulence model in the present study. In order to simulate the turbine in the moving reference frame the Navier-Stokes equations were modified by adding an inertial term to the equation, and modifying the velocity Dirichlet boundary conditions. Two tests were conducted to vary each of the parameters of oscillation; the non-dimensional surge amplitude, $A^* = A/R$, and the non-dimensional frequency ratio, $\omega^* = \omega_o/\omega_R$, where $A$ and $\omega_o$ are the amplitude and frequency of surge oscillation, and $R$ and $\omega_R$ are the rotor radius and rotational frequency. These tests were conducted to study the effects of each parameters to the hydrodynamic performance of the tidal turbine. Result shows that stalling effects occur when the velocity relative to the rotor is at the maximum. In certain cases, negative thrust and power coefficients were found when the velocity relative to the rotor is at the minimum. The fluctuation amplitude of the loading increases together with the amplitude and frequency of oscillation, which will contribute to the fatigue on the rotor.

## Introduction

The present study focuses on the hydrodynamic performance of an offshore floating tidal turbine oscillating in surge motion. A 3-bladed horizontal axis tidal turbine, with a diameter of 20m, was chosen for the present study as this scale of turbine reflects commercial applications. The moving reference frame approach was used to simulate the surge motion of the turbine and the RANS *k-ω* SST model was used to provide turbulence closure.

## Methods

The surging motion of the floating turbine is modelled in the non-inertial (moving) reference frame, where the coordinate system is fixed at the rotor. The Navier-Stokes equations are modified following the generalised method presented by Li et al. [1] to account for the motion of a body as follows

$$\nabla . U = 0 \tag{1}$$

$$\partial U/\partial t + U(\nabla . U) = -\nabla p + \upsilon(\nabla^2 . U) + B \tag{2a}$$

$$B = \dot{\omega} \times X - \ddot{x} + \omega \times (\omega \times X) + 2\omega \times U_A \tag{2b}$$

where $U$ and $p$ are the velocity vector and pressure in the moving reference frame, $x$ is the translational displacement of the moving object in the inertial frame, $\omega$ is the angular frequency of the rotating object, $X$ is the position vector relative to the moving reference frame, and $U_A$ is the object's velocity relative to the moving reference frame. The ( $\dot{}$ ) and ( $\ddot{}$ ) represent the first and second time derivative (velocity and acceleration), respectively. The terms in Equation (2b), from left to right, are: acceleration due to the change in angular velocity, translational acceleration of the moving body, centrifugal acceleration, and Coriolis acceleration. For the present study, since the rotor is oscillating only in surge motion, only the second term was added into the Navier-Stokes equation. The corresponding far-field velocity Dirichlet boundary condition then becomes

$$U(t) = U_{ap}(t) = U_\infty - \dot{x}(t) \tag{3}$$

where $U_\infty$ is the unperturbed inflow velocity in the far-field, $U_{ap}(t)$ is the apparent velocity seen by the turbine, and $\dot{x}(t)$ is the velocity of the moving turbine in surge motion.

* Mohamad H. B. Osman.
*Email address*: mohamad.binosman@eng.ox.ac.uk

## Results

Three different surge amplitude ratios, $A^*$ = 0.05, 0.10, 0.15 were investigated, holding $\omega^*$ = 1.0 and $\lambda$ = 4.4 constant to investigate the effects of surge amplitude on turbine performance and loads. The result (Fig. 1) shows asymmetries at the peak of each cycle, indicating flow separation occurrence along the blade for higher $A^*$ cases when the rotor oscillates in the upstream direction, showing that the rotor goes to stall. The rotor produces negative thrust and power when oscillating in the downstream for the highest $A^*$ case, with the rotor acting like a propeller rather than as a turbine.

Three cases of $\omega^*$ = 0.7, 1.0, and 1.3 (chosen based on Zhang et al. [2] study) were simulated to study the effects of surge frequency on the turbine performance, where $A^*$ and $\lambda$ were kept constant (0.1 and 4.4, respectively). The result (Fig. 2) shows asymmetries at the peak of each cycle, indicating the occurrence of flow separation along the blade for higher $\omega^*$ cases when the rotor oscillates into the upstream.

## Conclusions

As the amplitude and frequency of oscillation increase, the unsteady loading on the rotor increases, which will contribute to the fatigue damage of the rotor. Stall and flow separation are seen to occur on the rotor at maximum apparent velocity. The rotor can produce negative thrust and power coefficients at minimum apparent velocity for cases of large amplitude and frequency of oscillation.

*Acknowledgements:*

The authors would like to thank Majlis Amanah Rakyat Malaysia (MARA) and Universiti Teknologi Malaysia (UTM) for financial support, and Oxford University Advanced Research Computing (ARCUS) for providing high performance computing system services.

*References:*

[1] Li, L., Sherwin, S. J., Bearman, P. W. (2002). A moving frame of reference algorithm for fluid-structure interaction of rotating and translating bodies. *J. Numerical Methods in Fluids*, **38**, 187-206.

[2] Zhang, L., Wang, S., Sheng, Q., Jing, F., Ma, Y. (2015). The effects of surge motion of the floating platform on hydrodynamics performance of horizontal-axis tidal current turbine. *J. Renewable Energy*, **74**, 796-802.

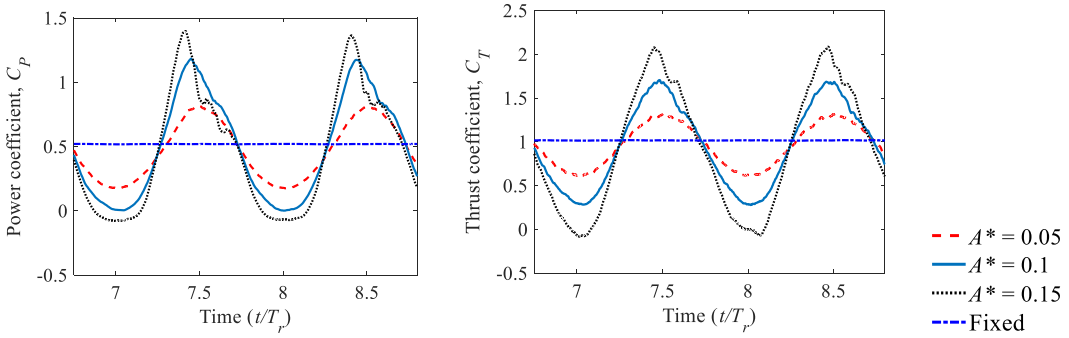


Fig. 1. Time histories of power and thrust coefficient for fixed and surging turbines at $A^*$ = 0.05, 0.10, 0.15 at fixed surge frequency, $\omega^*$ = 1.0, and tip-speed ratio, $\lambda$ = 4.4. $T_r$ is the turbine's rotation period.

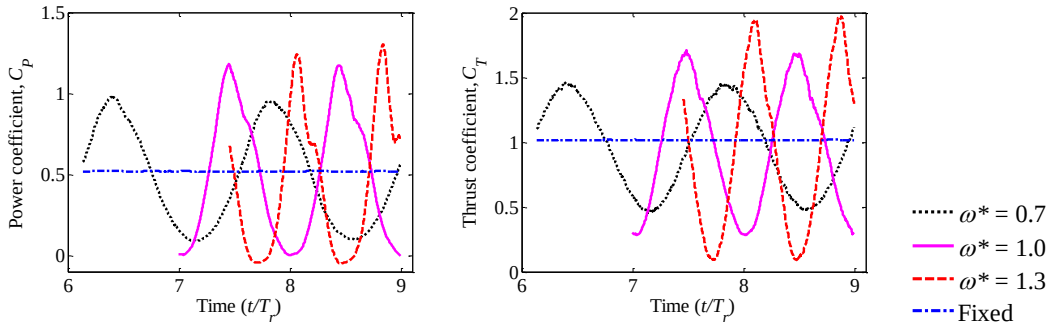


Fig. 2. Time histories of power and thrust coefficient for fixed and surging turbines at $\omega^*$ = 0.7, 1.0, and 1.3 at fixed oscillation amplitude, $A^*$ = 0.1, and tip-speed ratio, $\lambda$ = 4.4. $T_r$ is the turbine's rotation period.

# Sensor fusion and motion modelling of a floating tidal stream turbine

Thomas Lake*, Alison Williams, Ian Masters
*Marine Energy Research Group, Swansea University, UK*

*Summary:* As part of ongoing work to develop and validate a coupled floating body and tidal stream turbine model, the motion of a prototype floating tidal energy device was recorded between December 2017 and January 2018. Data from motion sensors have then been combined with GPS position using a Kalman filter based model, to provide an improved estimate of the platform's position and orientation. The results compare well with previously published work.

## Introduction

Floating tidal energy converters combine a floating support structure with a tidal energy converter, providing a method for deployment of tidal energy technologies which avoids directly mounting large devices to the seabed. Ongoing work at Swansea includes updating existing computational blade element momentum theory (BEMT) models to account for the motion of a floating support structure when calculating the power output and structural loading on the blades of a tidal stream turbine.

In support of this work, motion and operational data from the Sustainable Marine Energy (SME) PLAT-I platform has been recorded and analysed using the methods described below to extract position and orientation data for analysis and future use validating the updated BEMT model. The motion data also provides evidence of the stability characteristics of the platform.

## Methods

Data was collected using a combination of a commercial data logging and GPS unit with custom build inertial measurement units (IMUs) containing consumer motion sensors. This data has then been processed using a Kalman filter [1] with a simple model of platform motion represented with three degrees of freedom: a two-dimensional position and a heading. The use of a Kalman filter as part of the motion model allows information from different sensors to be combined to take advantage of their differing characteristics – e.g. using accelerometers to model changes in position between GPS updates. This class of filter can also be used to combine redundant sensors together into a single, more reliable source. Although multiple sensors were fitted to the platform during the test deployment, the results here use the accelerometers, gyroscope and magnetometers of a single sensor combined with the GPS data for position.

## Results

For the purposes of this analysis, the platform was classified as being in one of three states:

1. Operating – with all four turbines generating
2. Parked – all four turbines in the water, but with brakes engaged
3. Turbines raised – a maintenance state where the turbines are lifted out of the water

Each of these states yields different behaviour with regards to the position and orientation of the platform, as shown in figures 1 and 2. The results shown are based on data recorded during testing at Falls of Lora in Connel, Scotland between December 2017 and January 2018 [2]. Data was limited to a 1Hz timeseries for all sensors, with the mean value over 1 second taken as input when a higher sample rate dataset was available.

This behaviour has also been described previously in [2,3] using data gathered by SME. The position data recorded and modelled here is consistent with their results but is the result of independent analysis from a separate set of sensors. The heading data presented in figure 2 shows that the platform is generally aligned with the flow - principally west to east on the flood and east to west on the ebb, with generation limited to the ebb phase of the tide.

* Corresponding author.
*Email address*: t.lake@swansea.ac.uk

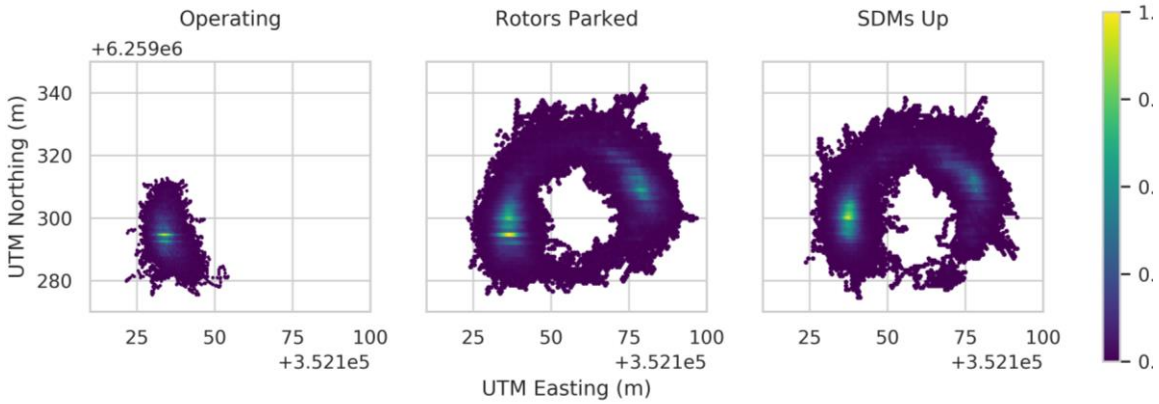


Fig. 1. Distribution of modelled position of the platform under different operating conditions

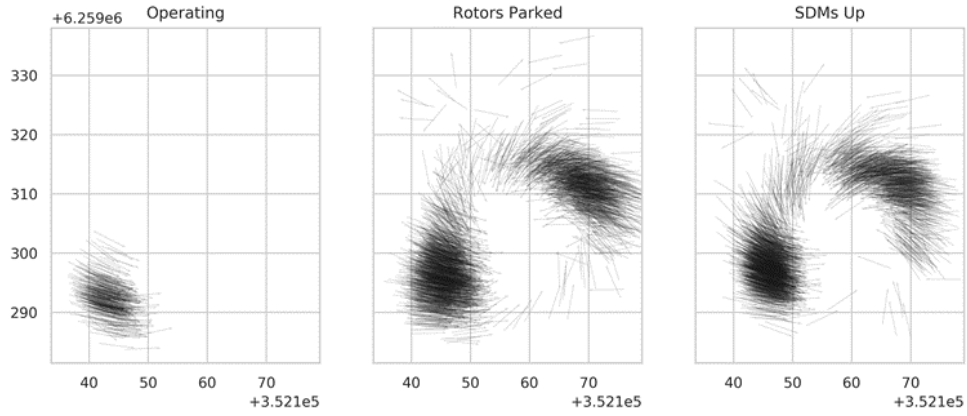


Fig. 2. Orientation of the platform under different operating conditions, based on two-minute averages

## Conclusions

The results obtained to date demonstrate the ability to track the position and orientation of a floating tidal platform over a multiple-month deployment. Further work to follow from these preliminary results will include extending the model to combine information from the additional sensors, and to extend the model to account for additional degrees of freedom (including pitch and roll). These results will then be compared to results from a combined BEMT and floating platform model in order to validate the behaviour of the combined simulation. PLAT-I has been redeployed at Grand Passage, Nova Scotia since collecting the data for the results presented here – applying this model to the new data received will also be carried out.

*Acknowledgements:*

The authors would like to thank Sustainable Marine Energy for allowing the use of their platform to collect the data presented here, and their ongoing support with future work.
This work was supported in part by the EPSRC under grant EP/N02057X/1

*References:*

[1] R. E. Kalman, “A new approach to linear filtering and prediction problems,” Journal of Basic Engineering, vol. 82, no. 1, p. 35, 1960.

[2] R. Starzmann, I. Goebel, and P. Jeffcoate, “Field performance testing of a floating tidal energy platform - part 1: Power performance,” in Asian Wave and Tidal Energy Conference, 2018.

[3] P. Jeffcoate and N. Cresswell, “Field performance testing of a floating tidal energy platform - part 2: Load performance,” in Asian Wave and Tidal Energy Conference, 2018.

# Validating a Numerical Model for Assessing Entire Floating Tidal Systems

Edward Ransley*, Scott Brown, Nan Xie, Deborah Greaves
*School of Engineering, University of Plymouth, UK*

Eamon Guerrini
*Modular Tide Generators (MTG)*

*Summary:* This paper presents the physical validation of a numerical model, based on the OpenFOAM CFD software. The model is designed to assess the complex coupled-nature of entire floating tidal stream concepts, including floating platform, catenary mooring system and on-board, submerged tidal turbine. Simulations of the Modular Tide Generators (MTG) floating tidal platform concept are compared with a series of 1:12 scale physical experiments, conducted in the COAST laboratory's Ocean Basin at the University of Plymouth.

## Introduction

Floating systems provide an opportunity to increase the available tidal energy resource and reduce the costs by reducing limitations on viable sites, accessing greater flow speeds near the free-surface and simplifying installation and maintenance processes. However, the close proximity of the free-surface raises concerns over the power delivery and survivability of these devices due to the presence of waves and the associated excitation of the floating structure. This has led to the development of a coupled and fully-nonlinear numerical model within the open-source computational fluid dynamics (CFD) software, OpenFOAM, which is capable of assessing the performance and behaviour of floating tidal concepts without decoupling the key parts of the system or over-simplifying the hydrodynamics involved. This paper presents validation of the numerical model through simulation of the Modular Tide Generator's (MTG) floating tidal platform concept, which consists of a catamaran style platform, catenary mooring system and a submerged horizontal axis tidal turbine (HATT) (Figures 1 and 2). The results are compared with a series of 1:12 scale physical experiments, conducted in the COAST laboratory's Ocean Basin at the University of Plymouth. The behaviour of the full system has been explored in a range of wave, current, and wave-current conditions, both with and without the turbine installed.

## Methods

The numerical model [1] is a fully nonlinear, coupled model, based on the open-source CFD libraries of OpenFOAM. The model solves the incompressible Reynolds-Averaged Navier-Stokes (RANS) equations for a two-phase fluid using expression based boundary conditions for wave/current generation and the 'relaxation zone' formulation for wave absorption [2]. Rigid-body motion is achieved, in six degrees of freedom, using the standard dynamic mesh deformation library which is combined with a new two-way coupled turbine library that calculates the additional loads from the turbine using a body-force implementation. In the cases considered here, turbine loads are approximated using actuator disc theory, reverse engineered to give the free-stream velocity as a function of the 'local' velocity in the region occupied by the turbine [1]. A recently developed mooring line library, based on the static catenary equations [3], has been used to simulate the four-point mooring system (Figure 1).

Physical experiments of the MTG concept [4] were carried out in the Ocean Basin of the COAST Laboratory at the University of Plymouth, UK. A 1:12 scale model of the device was constructed according to Froude similarity (with respect to the full-scale prototype design) with the submerged turbine being approximated using a porous disc (calibrated to give a similar thrust coefficient ($C_t \approx 0.82$) as that corresponding to the proposed 4m diameter HATT) (Figure 2). To allow an incremental validation of the numerical model, the experimental program consisted of a series of fixed tests, in which the model was fixed to the gantry above the basin via a 6-axis load cell, and moored tests, in which the model was floating and restrained by four catenary mooring chains.

This work focuses on a single wave frequency (0.78Hz), as this was found to be coincident with the peak frequency of pitch motion [4] and hence is considered to be a key design limit case for the MTG device. At model scale, the waves are 0.044m in height, are generated in a water depth of 1m, and are superimposed onto a current speed of 0.236m/s in the wave-current cases.

* Corresponding author.
*Email address*: edward.ransley@plymouth.ac.uk

## Results

The numerical model is shown to be capable of capturing some of the coupled behaviours: the nonlinear heave motion; the mean surge offset caused by thrust on the turbine, and; the increase in the mean total mooring load. The model also captures the motion-thrust coupling, predicting a similar relative increase in turbine thrust when moving from a fixed to a moored system. This coupling is key to the development of floating tidal devices due to the implications on both turbine fatigue and power delivery, and could influence the design of mooring systems in the future. Despite this, the predicted mooring loads show discrepancies in amplitude and some high-order effects are not captured. Furthermore turbine thrust is consistently over-predicted in wave-only cases. It is believed that the static catenary approach and 'steady' actuator-theory used are responsible for the discrepancies. It is anticipated that, including a dynamic catenary formulation, hydrodynamic drag on the mooring lines and a modified dynamic response method, for the turbine, will improve the model's predictive capabilities significantly.

## Conclusions

The numerical model presented generally performs acceptably in the cases considered here, and predicts that the motion of a floating system is a key consideration when assessing turbine power delivery and fatigue. However, the model requires further improvements, to provide a robust design tool, including dynamic formulations for both the catenary mooring system and turbine model.

*Acknowledgements:*

This work was funded as part of Innovate UK Project 103499 via the Industrial Strategy Fund. The authors would like to acknowledge the technical staff of the COAST Laboratory, particularly Dr Kieran Monk who contributed significantly to the model build and delivery of the physical experiments. The code presented here is available through the Collaborative Computational Project in Wave Structure Interaction (CCPWSI) [EP/M022382/1], which aims to bring together the community of researchers, data, code and expertise within the area of wave structure interaction (WSI) (https://www.ccp-wsi.ac.uk).

*References:*

[1] Brown, S.A., Ransley, E.J. and Greaves, D.M. (n.d.). Development of a turbine methodology for fully nonlinear, coupled modelling of floating tidal stream concepts, *under review*.

[2] Jacobsen, N.G., Fuhrman, D. and Fredsøe, J. (2012). A wave generation toolbox for the open-source CFD library: OpenFOAM, *International Journal for Numerical Methods in Fluids*, **70**, pp. 1073–1088.

[3] Bruinsma, N., Paulsen, B.T. and Jacobsen, N.G. (2018). Validation and application of a fully nonlinear numerical wave tank for simulating floating offshore wind turbines, *Ocean Engineering*, **147**, pp. 647–658.

[4] Xie, N., Ransley, E.J., Brown, S.A., Greaves, D.M., Nicholls-Lee, R., Johanning, J., Weston, P., Guerrini, E. (2018). Wave tank experiments of a floating, tidal-stream energy device, in *Proceedings of the 3rd International Conference on Renewable Energies Offshore (RENEW2018)*, Lisbon, Portugal

[5] Ransley, E.J., Brown, S.A., Xie, N., Greaves, D.M., Nicholls-Lee, R., Johanning, J., Weston, P., Guerrini, E. (2018). Concept development for deployment of a modular, floating, tidal stream device, in *Proceedings of the 3rd International Conference on Renewable Energies Offshore (RENEW 2018)*, Lisbon, Portugal

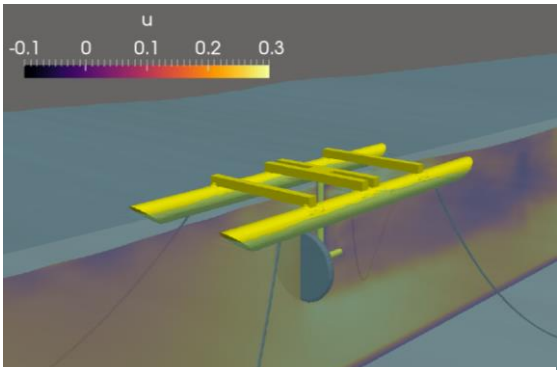


Figure 2: Numerical visualisation of the platform, moorings, turbine region and effect on the fluid.

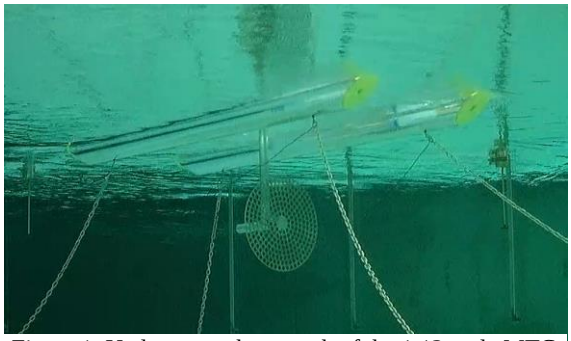

Figure 1: Underwater photograph of the 1:12 scale MTG model.

# Theoretical prediction of the efficiency of very large turbine arrays: combined effects of local blockage and wake mixing

Takafumi Nishino*
*Department of Engineering Science, University of Oxford, UK*

Scott Draper
*University of Western Australia, Australia*

*Summary:* We propose an extended theoretical model to predict the efficiency of a large number of aligned or staggered rows of turbines. The model is based on the actuator disc theory but now employs a hybrid inviscid-viscous approach to account for the effect of wake mixing between adjacent turbine rows. The model predicts, for staggered rows of turbines, the existence of an optimal mixing rate (and therefore, optimal row spacing) as a function of the local blockage of each turbine row. This array model may be coupled with a regional-scale flow model to predict the power of large tidal farms and, with some future modifications, large wind farms.

## Introduction

The effect of the arrangement of turbines has been the subject of many studies in both wind and tidal energy research. For tidal, Draper and Nishino [1] have extended the laterally confined actuator disc model of Garrett and Cummins [2] (hereafter GC07) to compare the efficiency of a single row and two aligned or staggered rows of turbines. Now we further extend this theoretical quasi-1D flow model to explore the efficiency of many rows of turbines; this is mainly for tidal applications but may also be useful for wind applications in the future.

## Theoretical model

We consider many rows of ideal turbines spaced equally and extending across the entire cross-section of a straight flow passage, like those considered in the tidal farm model of Vennell [3]. The number of rows is large enough to assume that the flow through the rows is fully developed, i.e. the velocity field around a turbine in a given row is identical to that in another row (except for the first few rows, which are outside the scope of this study but may be modelled separately). The cross-sectional positions of the turbines are either perfectly aligned or perfectly staggered (i.e. aligned for every two rows); a schematic of the latter case is shown in Fig. 1.

In the previous two-row model [1] the upstream conditions of the second row were determined directly from the downstream conditions of the first row without taking into account the effect of wake mixing. In this study we introduce a viscous mixing zone between each row (cf. Fig. 1*a*) and a new parameter, $m$ ($0 \le m \le 1$), which represents the 'completeness' of mixing within each viscous zone (defined such that $u_{out} = m u_{av} + (1-m) u_{in}$ at each cross-sectional position, with $u_{out}$ and $u_{in}$ being the velocities at the outlet and inlet of the viscous zone and

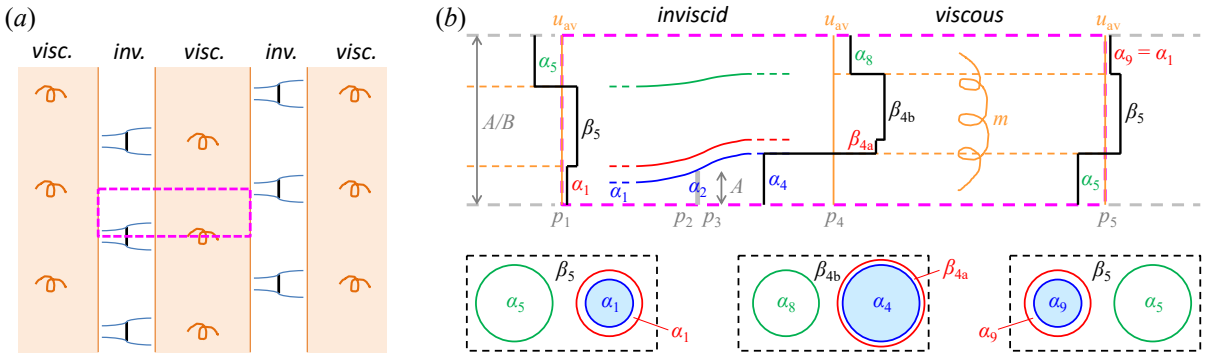


Fig. 1. Hybrid inviscid-viscous approach for very large turbine arrays: (*a*) sketch of a fully-developed part of the flow past a large number of staggered rows of turbines, divided into inviscid- and viscous-flow zones; and (*b*) diagram of a quasi-1D flow model for a staggered case with $B = 0.2$ and $m = 0.7$ (top) together with an example of how cross-sectional flow patterns may appear in a corresponding 3D flow problem (bottom).

* Corresponding author.
*Email address*: takafumi.nishino@eng.ox.ac.uk

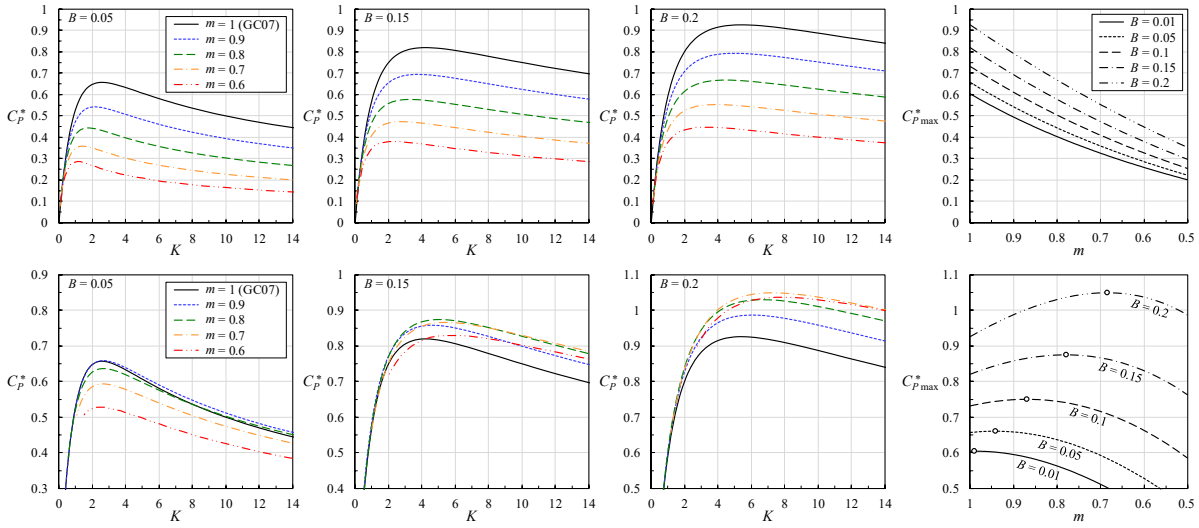


Fig. 2. Examples of the power coefficient, $C_P^*$ (plotted against the resistance coefficient, $K$) and its maximum value, $C_{P\,\max}^*$ (plotted against the mixing rate, $m$) for aligned turbines (top) and staggered turbines (bottom).

$u_{\mathrm{av}}$ the cross-sectional average velocity). We also assume that the bypass flow immediately outside of the core flow (with the velocity coefficient $\beta_{4\mathrm{a}}$ and cross-sectional area $A_{\beta 4\mathrm{a}}$) is merged with the main bypass flow (with $\beta_{4\mathrm{b}}$ and $A_{\beta 4\mathrm{b}}$) such that $\beta_5 = m\psi + (1-m)(\beta_{4\mathrm{a}}A_{\beta 4\mathrm{a}} + \beta_{4\mathrm{b}}A_{\beta 4\mathrm{b}})/(A_{\beta 4\mathrm{a}} + A_{\beta 4\mathrm{b}})$, where $\psi$ is a non-dimensionalised cross-sectional average velocity. This assumption is a little arbitrary but makes it possible to determine the upstream conditions of each turbine row from the conditions at the outlet of the viscous zone (cf. Fig. 1*b*). Eventually, we can calculate, e.g., the power coefficient of each turbine, $C_P^*$ (defined using $u_{\mathrm{av}}$ as the reference flow speed) as a function of the local (cross-sectional) blockage ratio, $B$, resistance coefficient, $K$ (constant for all turbines) and the mixing rate, $m$, as shown in Fig. 2. At $m = 1$, both aligned and staggered cases agree with GC07 [2]. For the aligned cases, $C_P^*$ always decreases with $m$. For the staggered cases, however, $C_P^*$ tends to be maximised at a mixing rate of less than 1 (this trend has also been predicted by a set of large-eddy simulations of actuator discs not shown here for lack of space) and this optimal mixing rate tends to decrease as the local blockage increases.

## Discussion and conclusions

These results suggest the importance of considering local blockage and wake mixing in a combined manner for future array design. The power coefficient $C_P^*$ obtained from this array model is a 'local' power coefficient since, in the real world, the average flow speed $u_{\mathrm{av}}$ may change depending on the momentum balance at a larger scale (as discussed in [3] for large tidal farms and [4, 5] for large wind farms). To predict the power of a large turbine array in a given environment, this model needs to be embedded in a larger (regional-scale) flow model.

Finally, it should be noted that this is a quasi-1D model, even though Fig. 1*b* (top) has been drawn in a two-dimensional manner. While the main advantage is its simplicity (using only three parameters, namely $B$, $K$ and $m$, to define the flow), a limitation of this quasi-1D model is that it conceptually breaks down when turbines are not fully but partially submerged in the wake of upstream turbines; this situation may occur in real 3D problems especially when the local blockage ratio is higher than about 0.2 for the staggered case. To resolve this, it might be necessary to introduce (either 2D or 3D) shear flows as in the study by Draper et al. [6]. Such an extension might also be necessary to apply the present work to the modelling of large wind farms, where the local blockage ratio cannot be defined easily but the flow may still be locally accelerated due to the local blockage effect [7].

*References:*

[1] Draper, S., Nishino, T. (2014) Centred and staggered arrangements of tidal turbines. *J. Fluid Mech.* **739**, 72-93.
[2] Garrett, C., Cummins, P. (2007) The efficiency of a turbine in a tidal channel. *J. Fluid Mech.* **588**, 243-251.
[3] Vennell, R. (2010) Tuning turbines in a tidal channel. *J. Fluid Mech.* **663**, 253-267.
[4] Nishino, T., Hunter, W. (2018) Tuning turbine rotor design for very large wind farms. *Proc. Roy. Soc. A* **474**, 20180237.
[5] Nishino, T. (2018) Generalisation of the two-scale momentum theory for coupled wind turbine/farm optimisation. *25th National Symposium on Wind Engineering*, Tokyo, Japan, 3-5 December, pp. 97-102.
[6] Draper, S., Nishino, T., Adcock, T. A. A., Taylor, P. H. (2016) Performance of an ideal turbine in an inviscid shear flow, *J. Fluid Mech.* **796**, 86-112.
[7] Nishino, T., Draper, S. (2015) Local blockage effect for wind turbines. *J. Phys.: Conf. Ser.* **625**, 012010.

# Variations in the optimal design of a tidal stream turbine array with costs

Zoe L. Goss, Stephan C. Kramer, Alexandros Avdis, Colin J. Cotter, Matthew D. Piggott
*Department of Earth Science and Engineering, Imperial College London, UK*

*Summary:* Many potential sites for tidal stream based electricity generation may be characterised as a strait between an island and a semi-infinite landmass. Optimising tidal array designs for this generalisation of a typical tidal site allows us to investigate the impact that choice of functional has on the array design. Rather than optimising for power alone, penalty terms for the cost of turbines as well as reward terms for economies of scale can impact the optimal design greatly. It is shown that sensitivity to changes in these terms is greatest for mid-range break even powers.

## Introduction

Draper et al. [1] identified four generic coastal sites for tidal stream arrays; a strait between two infinite ocean basins, an enclosed bay, a headland, and strait between an island and a semi-infinite landmass. Peréz-Ortiz et al. [2] investigated the upper limits to power generation in the latter for a tidal fence. We have investigated a site with a similar setup except for the assumption of a wider array area where turbines may be freely placed. This model resembles a simplification of many potential tidal sites, including the Alderney Race, which contains the majority of the Channel Islands resource, with a maximum potential of 5.1 GW as the flow is accelerated between the Isle of Alderney and France [3].

Large scale arrays need advanced numerical tools to optimise the yields and aid array design, especially since the effects of global blockage are important when the flow is able to bypass the strait. Studies often design for power alone, which can lead to an overestimate in the optimal number of turbines, through adding costly devices to the design even if they only increase a small amount more power [4,5]. To account for this a breakeven power has been added to the functional, which is the amount each device would need to generate to cover the costs of installing it. However, if this is constant it ignores the benefits which economies of scale bring through assuming that the breakeven power is independent of the number of turbines. To investigate this issue the breakeven power can be made to decrease linearly with the number of turbines.

## Methods

*Thetis* [6], a coastal ocean modelling package using the *Firedrake* finite-element code generation framework, is used to solve the flow through a channel with the nonlinear shallow water equations on an unstructured triangular mesh. The model geometry replicates the flow past a circular island setup used by Peréz-Ortiz et al. [2] as described in Fig. 1. A free slip condition is prescribed on the solid boundaries $\Gamma_2$, $\Gamma_3$ and $\Gamma_5$, and the open boundaries $\Gamma_4$ and $\Gamma_1$ have zero surface elevation and free surface elevation with M2 tidal forcing, respectively. The forcing takes the form $\delta_1 = a_0 a\sin(\omega_t t)$, with amplitude $a = 3\text{m}$ and frequency $\omega_t = 1.41 \times 10^{-4}\,\text{rad/s}$ and $a_0 = \left(1 - \cos(\omega_t t/4)\right)$ is used to ramp up the tidal signal over the first two tidal cycles.

Adjoint optimisation is used to optimise the continuous turbine density [7] across the array area, which can be converted into a discrete number of 16m diameter turbines. The functional was varied through a range of different breakeven powers, from $P_{BE} = 0\text{kW}$ (optimising for power alone) to $800\text{kW}$. The breakeven powers were also set to linearly decrease with number of turbines, to represent the economies of scale that may be achieved for larger scale arrays. The scaled breakeven power can be described as $P_{BE:es} = P_{BE} - es \cdot n_t$, where es is a coefficient for economies of scale, tested for $es = 0.05,0.1,0.15,0.2$. The functional $J = P_{avg} - P_{BE} \cdot n_t + es \cdot {n_t}^2$ is thus used, where $P_{avg}$ is the time-averaged power generated by the whole array.

## Results

Fig. 2 shows the time-averaged power generated by the whole array, the average power generated per device and the number of turbines variation against $P_{BE}$ and es. As $P_{BE}$ increases, the total power generated by the array decreases, while the power generated per device increases. The optimal $n_t$ decreases and, as Fig. 3 shows, the location of the remaining turbines transitions from being spread across the majority of $A_f$ into the region with the fastest flows - closest to the island. Additional details can be found in [8].

As es is increased, the total power generated and number of turbines increases, however the power generated per device decreases. As the effects of economies of scale are realised it becomes cheaper to add more turbines and therefore less important that each turbine is generating a high amount of power to balance out the diminished costs. However, for high and low $P_{BE}$ the impact that changing es has on the design is negligible. Since the effect that es has on the functional is proportional to ${n_t}^2$ this is unsurprising for designs with high $P_{BE}$ and low $n_t$ but it is unexpected for designs with low $P_{BE}$ and high $n_t$.

## Conclusions

The results show that optimal array design is greatly dependent on the breakeven power ($P_{BE}$) and the importance placed on power generation maximisation vs cost minimisation. However, in the scenario considered here, the array properties are found to be more sensitive to changes in the region $300\text{kW} \leq P_{BE} \leq 500\text{kWW}$. As $P_{BE}$ is decreased more turbines can be afforded in the optimal design and they spread out further South, while maintaining maximal density closest to the island: The array behaves as a barrage or fence and exploits blockage control. As this qualitative shift occurs, sensitivity to other small changes in the functional, such as variation in economies of scale, become pronounced. Array designers should be aware of this region of greater sensitivity when trying to evaluate the impact of uncertainty on the optimal design.

*Acknowledgements:*

Z. L. Goss acknowledges the support of the Engineering and Physical Sciences Research Council Centre for Doctoral Training in Mathematics of Planet Earth [grant number EP/L016613/1]. M. D. Piggott acknowledges the support of EPSRC under grants EP/M011054/1 and EP/R029423/1.

*References:*

[1] S. Draper, T. A. Adcock, A. G. L. Borthwick, and G. T. Houlsby, "Estimate of the tidal stream power resource of the Pentland Firth," Renewable Energy, vol. 63, pp. 650 – 657, 2014.

[2] A. Pérez-Ortiz, A. G. L. Borthwick, J. McNaughton, H. C. Smith, and Q. Xiao, "Resource characterization of sites in the vicinity of an island near a landmass," Renewable Energy, vol. 103, pp. 265 – 276, 2017. Available: http://www.sciencedirect. com/science/article/pii/S0960148116309740

[3] D. S. Coles, L. S. Blunden, and A. S. Bahaj, "Assessment of the energy extraction potential at tidal sites around the Channel Islands," Energy, vol. 124, pp. 171 – 186, 2017.

[4] Z. L. Goss, M. D. Piggott, S. C. Kramer, A. Avdis, A. Angeloudis, and C. J. Cotter, "Competition effects between nearby tidal turbine arrays-optimal design for Alderney Race," Renew, 2018

[5] Z. L. Goss, M. D. Piggott, and S. C. Kramer, "An English Channel Model for the Optimisation of Tidal Turbines in the Alderney Race," OTEW, 2018.

[6] T. Kärnä, S. C. Kramer, L. Mitchell, D. A. Ham, Matthew D. Piggott, and A. M. Baptista. "Thetis coastal ocean model: Discontinuous Galerkin discretization for the three-dimensional hydrostatic equations. Geoscientific Model Development", 11(11):4359–4382, 2018.

[7] S. W. Funke, S. C. Kramer, and M. D. Piggott. "Design optimisation and resource assessment for tidal stream renewable energy farms using a new continuous turbine approach". Renewable Energy, 99:1046 – 1061, 2016.

[8] Z. L. Goss, S. C. Kramer, A. Avdis, C. J. Cotter, and M. D. Piggott, "Economic optimisation of large scale tidal stream turbine arrays," EWTEC, 2019

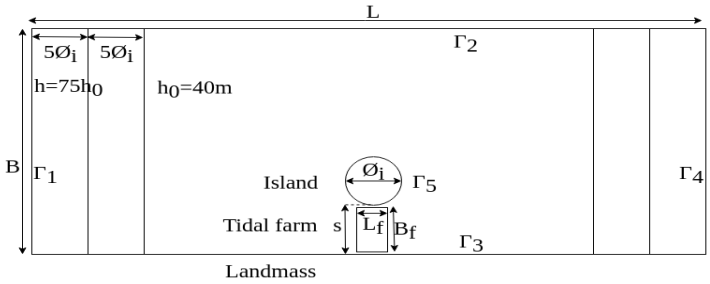


Fig. 1. Geometry for an idealised model of flow through a channel with an island of diameter Øi = 2000m and a tidal site of area Af = Bf × Lf where turbines can be added. The depth is increased linearly from $h_0$ to $75h_0$ to mimic the conditions at the continental shelf.

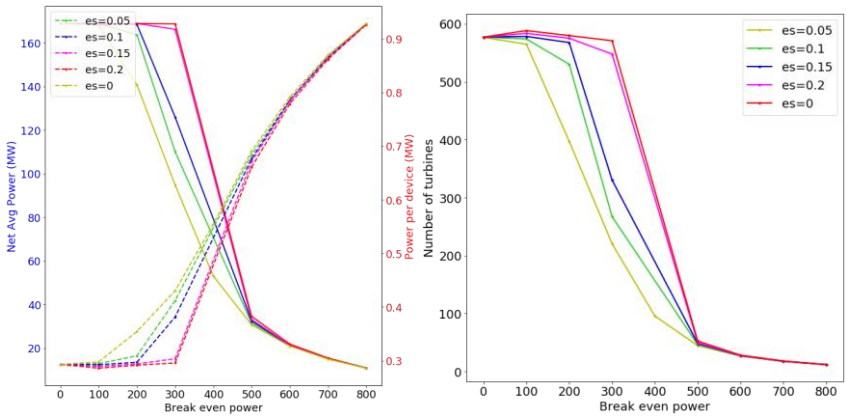


Fig. 2. Variations in the average power generated and the number of turbines for the optimal design as $P_{BE}$ and $es$ are increased.

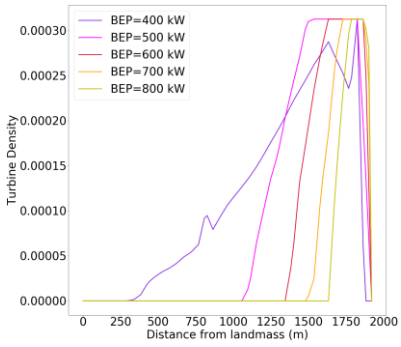


Fig. 3. The optimal turbine density along the vertical centre line (from 0m from the Southern Landmass to 2000m at the most Southern part of the island) of the array as $P_{BE}$ and $es$ are increased.

# A Speed Control Strategy for Parallel Connected Tidal Turbines in an Array Using a Variable Ratio Drive

Simon Reynolds*[1], Aristides Kiprakis[1] and Mohammad Abusara[2]
[1] *School of Engineering, The University of Edinburgh, UK*
[2] *University of Exeter, Penryn, UK*

*Summary:* Shared export cables in conjunction with onshore converters has the potential to reduce the cost of energy generated by tidal turbine arrays. A key challenge to the implementation of this configuration is to successfully control multiple parallel connected generators whilst still optimising rotor performance over a range of varying flow speeds. A control strategy is proposed for use with a variable ratio drive to overcome this difficulty and validated using a Simulink model, with initial results suggesting it provides a viable solution.

## Introduction

Export cables make up a significant proportion of the upfront material and installation costs for tidal turbine arrays. Reducing cable numbers would lower the cost of energy generated by an array, thereby improving commercial viability. This could be achieved by operating the generators of multiple turbines in parallel via shared export cables. In addition, the power conversion equipment required to convert the output from an induction generator into grid ready electricity is relatively failure prone [1]. Operating expenditure can be reduced by locating this equipment onshore, further lowering the cost of energy produced. Combining these two proposals poses a control challenge, since parallel generators must maintain their stator frequencies in phase for operation via a shared export cable and onshore converter. This is difficult to achieve when turbines are subjected to spatially and temporally varying flow speeds, without operating their rotors away from optimal Tip Speed Ratio (TSR). To maintain peak TSR and minimise slip differences between parallel generators, divergence in generator rotor frequencies can be reduced with a variable ratio drive, e.g. the Voith Vorecon /WinDrive [2]. A Simulink model was built to initially validate a proposed control strategy for this arrangement.

## Methods

The Simulink model focussed on determining the necessary range of operation for the variable ratio drive and dynamically calculating the reference torque value required for the induction generator. The strategy used is explained visually in Fig. 1, with the limits of the Simulink model shown. A 12 hour flow regime was created (Fig. 2) using data obtained in Ramsey Sound from Acoustic Doppler Current Profiler (ADCP) measurement [3].

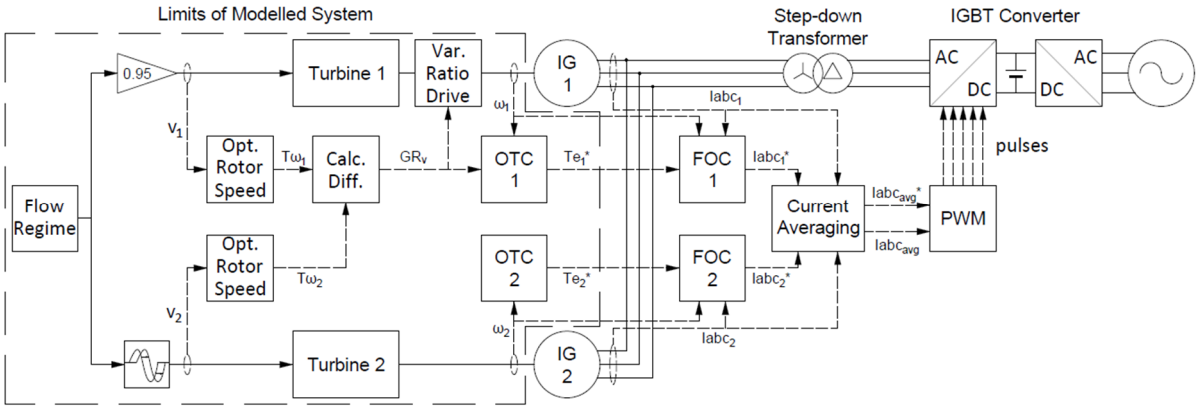


Fig. 1 Control Strategy Schematic with Simulink Model Limits Shown

The flow regime was sent to two turbine blocks, one seeing a 2 second delay and one having a 5% reduction. Optimum rotor speeds ($T\omega_x$) were calculated for each based on flow speeds ($v_x$) and the difference calculated to obtain the gear ratio ($GR_v$) required to maintain the same generator speed ($\omega_x$) despite differing rotor speeds. Gear ratio and generator speeds were also used to calculate the reference generator torque ($Te_x^*$) needed for an electrical control strategy using a torque gain term ($k_{TSR}$) derived via Optimal Torque Control (OTC) [3]:

$$Te_x^* = \omega_x^2 \times k_{TSR} \ (Nm) \tag{1}$$

* Corresponding author.
*Email address*: s.reynolds@ed.ac.uk

$$k_{TSR}=0.5\times\rho\times\pi\times R^5\frac{C_p{}^{max}}{TSR^{max3}\times\left(GR_f/GR_v\right)^3} \quad (2)$$

Where: ρ = fluid density = 1025 kg.m$^{-3}$; R = turbine radius = 6m; $C_p{}^{max}$ = maximum $C_p$ = 0.40481; $TSR^{max}$ = maximum TSR = 3; $GR_f$ = fixed gearbox ratio = 72.

## Results

Results generated from the Simulink model provided initial validation that the control strategy can match generator speeds using a sensible range of ratios (Fig. 4) for a variable ratio drive, whilst allowing the rotors to operate at their optimal speed for a given flow (Fig. 3). Generator reference torque was also calculated (Fig. 5); which would be sent to the Field Oriented Control (FOC) scheme before a current averaging calculation would generate control pulses for the parallel connected generators via Pulse Width Modulation (PWM).

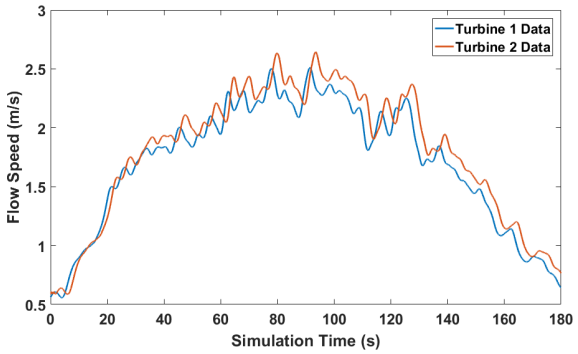


Fig. 2 Flow Speed vs. Simulation Time

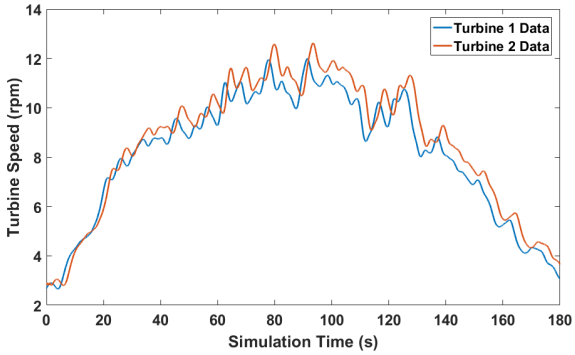


Fig. 3 Turbine Speed vs. Simulation Time

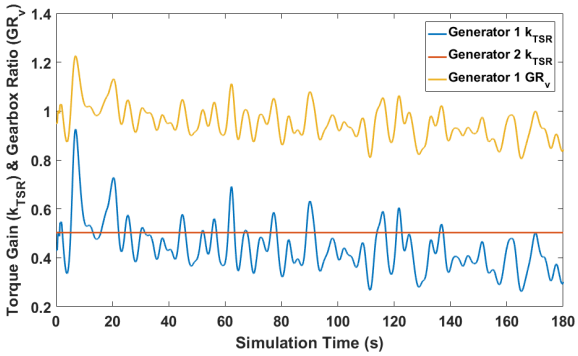


Fig. 4 $k_{TSR}$ & $GR_v$ vs Simulation Time (s)

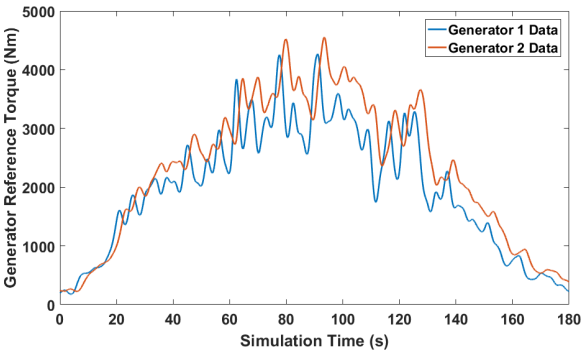


Fig. 5 Generator Ref. Torque vs. Simulation Time (s)

## Conclusions

A control strategy proposed for speed matching of parallel connected generators using a variable ratio drive was validated using a Simulink model. The range of ratios used to match generator speed was found to be within sensible limits for existing technology. A torque gain term calculation method was derived and subsequently used to establish the required generator reference torque for an electrical control strategy. Crucially, both turbine rotors were able to operate at their optimum speed despite different tidal flows, thereby maximising efficiency.

*Acknowledgements:*

The authors would like to thank the IDCORE Programme and the University of Edinburgh for funding this project in conjunction with the ETI and the RCUK Energy programme (Grant number EP/J500847/1).

*References:*

[1] Delorm, T. M., Zappala, D. & Tavner, P. J., 2012. Tidal stream device reliability comparison models. *Journal of Risk and Reliability*, Proceedings of the Institution of Mechanical Engineers, 226(6), pp. 6 - 17.

[2] Voith Turbo GmbH & Co. KG, 2018. Variable Speed Drives. [Online] Available at: https://voith.com/corp-en/drives-transmissions/variable-speed-drives.html

[3] Titan Environmental Surveys Ltd, 2012. CS0332 Ramsey Sound ADCP Final Report, Bridgend: Titan Environmental Surveys Ltd.

[4] Yaramasu, V. & Wu, B., 2017. Model Predictive Control of Wind Energy Conversion Systems. 1st ed. Hoboken: John Wiley & Sons Inc.

# Blade-Explicit Fluid-Structure Interaction of a Ducted High-Solidity Tidal Turbine

Mitchell G. Borg, Qing Xiao*, Atilla Incecik
*Department of Naval Architecture, Ocean, and Marine Engineering, University of Strathclyde, UK*

Steven Allsop, Christophe Peyrard
*EDF R&D (Electricité de France Research & Development), Chatou, France*

*Summary:* This work elaborates a computational fluid dynamic (CFD) model utilised in the investigation of the structural performance concerning a ducted high-solidity tidal turbine in aligned and yawed inlet flows. Analysing the hydrodynamic performance at aligned flows portrayed the distinctive power curve at which energy is transferred via the fluid-structure interaction. At distinct bearing angles with the axis of the turbine, variations in the blade-interaction due to the presence of the duct was acknowledged within a limited angular range at distinct tip-speed ratio values. As a result of the hydrodynamic analysis, a structural investigation of the blades was discretely evaluated in an effort to acknowledge fluid-structure phenomena.

## Introduction

Effectively harnessing the power of the ocean for sustainable energy generation is an incredible feat. In an effort to increase the capacity of energy-generating systems, design altercations have been in constant assessment and development, with a plethora attaining implementation within the global market. On the forefront of the pertinent research in achieving this endeavour is the increase of mass flow through the turbine, together with the alignment of the flow to facilitate further turbine installations. As a result of the development attained, ducts have been installed along the perimeter of rotors to attain an increase in power exchange [1, 2]. The numerical analysis elaborated in this study describes a real-scale CFD model developed to assess the hydrodynamic performance of a high-solidity open-centre tidal turbine within a bidirectional duct in flows at aligned and angular bearings. In continuation of analysing the fluid-structure effects, the structural mechanics of blades was analysed by employment of Finite Element Analysis (FEA), in effort of comprehending the physics induced by the duct.

## Methods

In continuation to Borg et al. [3, 4], the CFD models were solved by means of ANSYS Fluent 18.0, where the physical models were designed to consist of a domain layout imposed with relevant boundary conditions. The CFD solver was utilised to compute the Reynolds-averaged conservation equations as time-averaged representations of the continuity and momentum equations which govern the three-dimensional, unsteady, incompressible fluid flow. The domain surrounding the turbine was segregated from the global domain to induce a moving mesh model with rotation at the turbine. Closure of the Unsteady Reynolds-Averaged Navier-Stokes (URANS) equation was modelled by means of the RSM turbulence model due to its superiority in analysing anisotropic flows.

In an effort to attain a validated CFD model for tidal turbine applications, simulations were established to replicate the experimentation undertaken by Mycek et al. Identical blade, nacelle, and mast geometry were utilised within the model domain; the parameters of the turbine and fluid flow were also instated from the literature. Upon validation, the model settings were implemented for the analysis of a ducted eight-bladed tidal turbine, similar to the design of the OpenHydro PS2 device, illustrated in Figure 1. The turbine geometry was implemented within the model domain. Similar to the validation, the physical model was designed to consist of identical domain layout and boundary conditions as the three-bladed horizontal-axis tidal turbine (HATT). The parameters of the turbine and fluid flow were instated from real-world data, provided by EDF R&D. Subsequent to the hydrodynamic analysis, the pressure distribution along the blade surfaces in variation with elapsed time, was exported from the CFD solver to the FEM solver. The structural parameters of the rotor blades were derived by means of literature with specific regards to the related layout and domain within which the turbine operates; utilising a transient analysis, the outcomes were deduced in an effort to acknowledge commissionable properties for operation.

* Corresponding author.
*Email address*: qing.xiao@strath.ac.uk

## Results

Consequent to the methodology, the resultant outcomes, in terms of power coefficient, thrust coefficient, and velocity profiles in the wake, were established for all simulation cases. Primarily, the three-bladed HATT CFD model outcomes were compared to literature. In comparison to the distinct curves, a similarity index of over 95% was acknowledged at the power coefficient plateau region, together with all CFD TSR data points falling within $2\sigma_{CP}$ with experimentation TSR data points, displaying good comparison, as illustrated in Figure 2.

Once the modelling techniques were implemented for the ducted turbine, unique outcomes were displayed. Notably, the TSR curve is relatively short spanning, with a TSR range of 1 – 2.5, which is characteristic of a high-solidity turbine. In this region, the peak power coefficient of 0.34 is achieved along with a decrease of 0.1 from its nominal TSR. In continuation, the implementation of the mechanical properties of the blades permitted the structural analysis to provide outcomes representing the deflections, principal stresses, and frequency in relation to fatigue investigations.

## Conclusions

This study put forward the concept of a numerical analysis of a ducted high-solidity open-centre tidal turbine in an effort to establish its hydrodynamic and structural properties in aligned and yawed flow. By means of CFD validation, the power output, thrust resistance, and maxima stresses within the ducted turbine were recognised to depict outcomes for a characteristic representation of the arrangement in real-ocean conditions.

*Acknowledgements:*

The research work disclosed in this publication is partially funded by the Endeavour Scholarship Scheme (Malta). Scholarships are part-financed by the European Union - European Social Fund (ESF) - Operational Programme II -- Cohesion Policy 2014-2020: "*Investing in human capital to create more opportunities and promote the well-being of society*".

Results were obtained using ARCHIE-WeSt High Performance Computer (www.archie-west.ac.uk).

*References:*

[1] C. Belloni, "Hydrodynamics of Ducted and Open-Centre Tidal Turbines," University of Oxford, Oxford, United Kingdom, 2013.
[2] S. Allsop, "Hydrodynamic modelling for structural analysis of tidal stream turbine blades," University of Exeter, Exeter, United Kingdom, 2018.
[3] Borg, M. G., Xiao, Q., Incecik, A., Allsop, S., and Peyrard, C., 2018. "Numerical Analysis of a Ducted High-Solidity Tidal Turbine". In OCEANS'18 MTS/IEEE Kobe, IEEE.
[4] Borg, M. G., Xiao, Q., Incecik, A., Allsop, S., and Peyrard, C., 2018. "An Actuator Disc Analysis of a Ducted High-Solidity Tidal Turbine", to be presented at ASME 2019 38th International Conference on Ocean, Offshore and Arctic Engineering OMAE 2019-96014

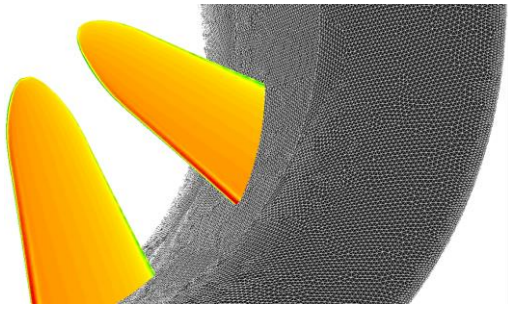

Figure 1 – Ducted High-Solidity Open-Centered Turbine in Representation of Pressure Contours

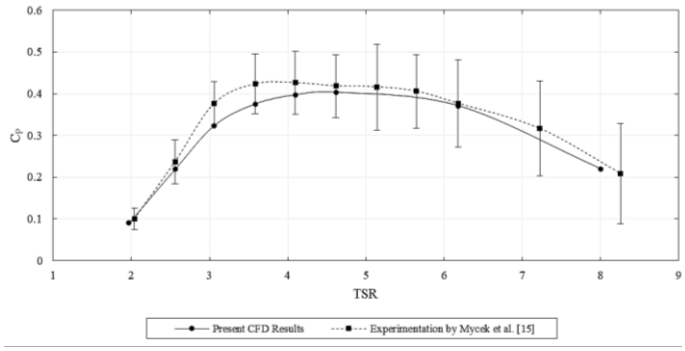


Figure 2 – Comparison of CFD and Experimentation Power Coefficient Results for Three-Bladed HATT [3]

# Analysis of unsteady loading of a tidal stream turbine with an Actuator Line RANS model

Wei Kang*[1,2]
David Apsley[1], Tim Stallard[1], Peter Stansby[1]
[1]*School of Mechanical, Aerospace and Civil Engineering, University of Manchester, UK*
[2]*School of Astronautics, Northwestern Polytechnical University, China*

*Summary:* Loading induced by the complex interaction of both turbulence of the onset flow and generated by a rotating turbine have a great impact on the operational reliability and lifespan of turbines. A RANS model for a single tidal turbine is established together with actuator line method to account for the rotating blade effect. Unsteady blade loading is also studied with different TSRs and turbulent parameters. The results show that the multiple peaks of the blade frequency agree well with experimental data in low and mid-frequency up to about $10f_0$, where $f_0$ the rotor frequency.

## Introduction

When tidal turbines are deployed and operating in narrow channels and straits, unsteady loading caused by the onset flow and generated by the turbine has a great impact on fatigue loading which defines the lifespan of turbines (Blackmore et al. 2011). Ahmed et al. 2017 compared RANS and LES for fluctuating loads on the blade of a single tidal turbine with turbulent inflow. The results show that the distribution of spectral energy at low to mid frequencies (in range $f_0$ to $10f_0$) can be associated with onset turbulence, which can be resolved by RANS simulation with suitable inflow. In this study, a tidal turbine model is established using RANS CFD method. Unsteady loading are evaluated with different tip speed ratios (TSRs) and turbulence parameters.

## Methods

The computation in this study is conducted using STREAM, an in-house finite-volume solver for (RANS) equations on multi-block, structured, curvilinear meshes using SIMPLE pressure-correction algorithm. k-ε turbulent model is used with standard wall function. The turbulent intensity is set 3% and 12%, respectively, to match experimental measurements, whilst turbulent viscosity ratio is set at ten. Rotor blades are represented by rotating actuator lines (Apsley et al. 2018), whilst the fixed support structure and nacelle are represented by partially-blocked-out cells. The aerodynamic data for the NACA63-8XX airfoil is obtained from Batten and Bahaj (2007). The force obtained for each actuator control point defines a momentum sink that is distributed using an exponential function and no explicit tip correction is considered. Numerical cases are simulated in the Parallel Computing cluster at the University of Manchester.

## Results

The computational model is derived from the experimental model described in Payne et al. 2017 and Payne et al. 2018, with a rotor diameter D=1200mm and mean flow velocity of 0.8m/s. The mean thrust and power coefficients for streamwise turbulence intensities of 3% and 12% are compared with the experimental data at various TSRs in uniform inflow profile, shown in Fig.1 (Blue: TI=3%, Red: TI=12%). It is seen that the thrust coefficients are overall slightly higher than the experimental data, while the power coefficients agree well for TSR<6 but are underestimated as the TSR increases to 7. Agreement with experiment is observed over a wider TSR range for the higher turbulence intensity case of 12%. Figure 2 compares spectral densities of root bending moment at TSR=7. The frequency is normalized by the rotating frequency of the rotor ($f_0$) and the power is normalized with mean square amplitude. The multiple peaks of the blade frequency agree well with experiment at low-mid frequency range $f / f_0 < 10$ but the magnitude is much greater beyond this range.

## Conclusions

A RANS model for a single tidal turbine is validated by the experimental data. The thrust coefficients is overall slightly higher than the experimental results, while the power coefficients agree well as TSR<6 but are

* Corresponding author. *Email address*: wei.kang@manchester.ac.uk

underestimated as the TSR increases to 7. Unsteady loading is also compared for different turbulence intensity values. The power spectrum extracted from a single blade has a broader range of harmonic rotating frequencies that share a similar trend with higher turbulence intensity. The multiple frequency peaks and magnitudes of root bending moment are in reasonable agreement with experimental data up to a frequency of approximately $10f_0$. Further work will be carried out to study the effects of time-varying onset flows due to coherent turbulent structures and surface waves.

*Acknowledgements:*

The authors would like to acknowledge the support of the EPSRC Supergen Offshore Renewable Energy Hub.

*References:*

[1]. Ahmed, U., D. D. Apsley, I. Afgan, T. Stallard and P. K. Stansby (2017). "Fluctuating loads on a tidal turbine due to velocity shear and turbulence: Comparison of CFD with field data." Renewable Energy 112: 235-246.

[2]. Apsley, D. D., T. Stallard and P. K. Stansby (2018). "Actuator-line CFD modelling of tidal-stream turbines in arrays." Journal of Ocean Engineering and Marine Energy 4(4): 259-271.

[3]. Blackmore, T., W. Batten, M. Harrison and A. Bahaj (2011). "The sensitivity of actuator-disc rans simulations to turbulence length scale assumptions." European Wave and Tidal Energy Conference.

[4]. Payne, G. S., T. Stallard and R. Martinez (2017). "Design and manufacture of a bed supported tidal turbine model for blade and shaft load measurement in turbulent flow and waves." Renewable Energy 107: 312-326.

[5]. Payne, G. S., T. Stallard, R. Martinez and T. Bruce (2018). "Variation of loads on a three-bladed horizontal axis tidal turbine with frequency and blade position." Journal of Fluids and Structures 83: 156-170.

[6]. Batten WMJ, Bahaj AS, Molland AF, et al(2007). “Experimentally validated numerical method for the hydrodynamic design of horizontal axis tidal turbines”. Ocean Engineering 34 (7): 1013-1020.

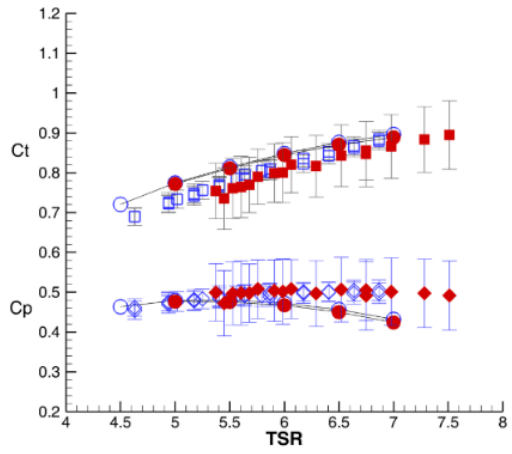


Fig 1 Comparison of thrust and power coefficient between computation (Circle) and experiment (Square/Diamond)

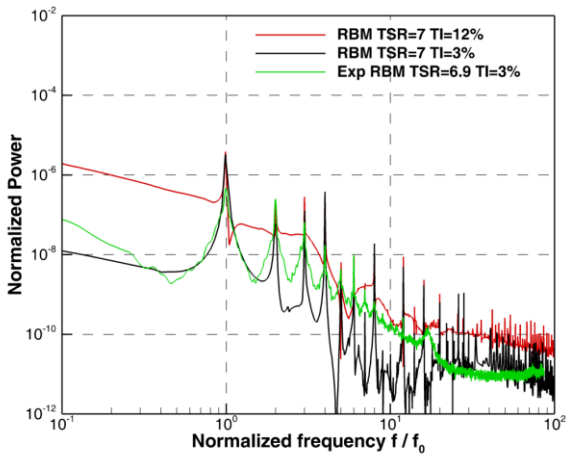


Fig 2 Comparison of spectral densities of root bending moment

# Numerical Modelling of a Vertical-Axis Cross-Flow Turbine

Ruiwen Zhao*, Angus Creech, Alistair Borthwick
*School of Engineering, University of Edinburgh, UK*

Takafumi Nishino
*Department of Engineering Science, University of Oxford, UK*

*Summary:* This paper presents a numerical model of a single vertical-axis turbine (VAT) with an arbitrary number of blades. This cross-flow turbine model is simulated within the OpenFOAM CFD framework using information from a modified version of the Wind and Tidal Turbine Embedded Simulator (WATTES) source code, called WATTES-V. The actuator line theory is used in WATTES-V to capture important flow features that contribute to the wake recovery behind a VAT.

## Introduction

An array of close-packed vertical-axis contra-rotating rotors has been designed by Stephen Salter to maximize the fraction of flow passage swept [1]. In this study we aim to model one of these tidal rotors to examine the vorticity magnitude distribution behind the rotor. Tip-loss effects and dynamic stall are to be incorporated in the model as corrections applied to the force terms in the actuator line method. It is believed that tip vortices caused by adjacent foils at different angles could be suppressed using the spoked-ring wheel. Proper pitch control could solve the problem of dynamic stall at a low tip speed ratio [1].

The WATTES [2, 3] code, an open library source code written in Fortran95 [4], is used to predict the dynamic response to the flow, where lift and drag force components are calculated from tabular aerofoil data. WATTES uses both the dynamic torque-controlled actuator disc method and the actuator line technique with active-pitch correction to model horizontal-axis wind and tidal turbines [2, 3]. A modification is made to WATTES to simulate a VAT, which is then coupled with OpenFOAM to investigate the wake of a VAT. The coupled OpenFOAM and modified WATTES-V model then enables active pitch control and blade-generated turbulence to be considered in the context of dynamic stall and tip-vortex losses in a future study.

## Methods

The actuator line method (ALM) [5] creates a distribution of body forces along a set of line segments representing the blades of a turbine. For each turbine, nodes are found within the control turbine volume, where the flow velocity relative to the blades $u_{rel}$ and angle of attack $\alpha$ are calculated from the local inflow velocity $u$, blade velocity $u_{bl}$, and azimuthal blade angle $\theta$ with the corrected blade pitch $\beta$. Lift $F_L$and drag $F_D$ forces are calculated with the Gaussian regularization $\eta_i(x)$ from ALM theory in order to obtain the torque terms (e.g. the torque on fluid $\tau_{fl}$, and the torque turns the generator to create power $\tau_{pow}$).

$$\overrightarrow{F_L} = \sum_{i=1}^{N_{bl}} \eta_i(x)\, \overrightarrow{f_{L_i}}, \qquad \overrightarrow{F_D} = \sum_{i=1}^{N_{bl}} \eta_i(x)\, \overrightarrow{f_{D_i}} \tag{1}$$

where $N_{bl}$ is the number of blades, $x$ is the distance from the ALM element quarter chord location, $\overrightarrow{f_{L_i}}$ and $\overrightarrow{f_{D_i}}$ are the nodal lift and drag respectively per unit span length for $i^{th}$ blade.

All the calculated force terms are passed back to OpenFOAM as the momentum sources in the Navier-Stokes momentum equation for an incompressible Newtonian fluid:

$$\frac{\mathrm{D}\vec{u}}{\mathrm{D}t} = -\frac{1}{\rho}\nabla p + \nu\nabla^2\vec{u} + \frac{1}{\rho}\vec{F} \tag{2}$$

where $\vec{u}$ is velocity field vector, $\rho$ is fluid density, $p$ is pressure, $\nu$ is fluid kinematic viscosity, $t$ is time, and $\vec{F}$ is the body force vector exerted on the fluid.

This VAT model is first validated against an experimental wind tunnel model of a two-bladed H-type VAWT equipped with sensors to measure thrust and side loading with respect to the turbine [6]. The experimental data were collected from a VAWT at the Open Jet Facility (a closed loop open jet test section in a wind tunnel) at

* Corresponding author.
*Email address*: r.zhao@ed.ac.uk

Delft University of Technology [6]. This VAT of solidity 0.1 was modelled using WATTES-V source code with ALM in conjunction with a Reynolds-averaged Navier-Stokes (RANS) simulation using the $k-\omega$ SST turbulence closure model in OpenFOAM. It should be noted the spoked-ring wheel of the modelled VAT is a more efficient load-bearing structure than a tower, which experiences vortex shedding and reduces the bending stresses of blades. Tip loss has been neglected in the present study, given that it is likely less significant in a vertical- than in a horizontal-axis turbine. Proper pitch control of the modelled VAT should solve the problem of dynamic stall, however, the tip-speed ratio used in the validation case is high enough to be outside the range in which dynamic stall would be likely to occur. The goal of this verification was to compare the thrust of turbine at different azimuthal angles.

## Results

Fig. 1 shows the velocity magnitude distribution in one horizontal plane. The flow field is complicated, owing to the presence of vortices that have shed from the blades and then advected in the turbulent wake. Fig. 2 depicts a comparison between the numerical results and the measured forces for a tip speed ratio of 3.7. The measurements have been averaged over 22 turbine rotations for a flow speed of 4.01 $m/s$ and a fixed pitch angle of $0^{\circ}$. It can be seen that the numerical predictions and measurements of the thrusts in both $x-$ and $y-$ directions are very similar in terms of amplitude and profile. In both the numerical and experimental results, the maximum blade loading occurs at the blade azimuth of $90^{\circ}$ and $270^{\circ}$.

## Conclusions

The numerical model of a single vertical-axis turbine (VAT), represented using actuator line theory, gives numerical predictions in satisfactory overall agreement with measured data on thrust on a two-bladed VAT. In future work, the blade pitch will be controlled to attain an even pressure drop along two rows of close-packed contra-rotating rotors and a parameter study undertaken to examine the effect of active pitch on wake turbulence.

*Acknowledgements:*

The first-named author is supported by funding partly from the China Scholarship Council, and partly from the University of Edinburgh. The authors thank Prof. Stephen Salter for providing helpful suggestions.

*References:*

[1] Salter, S. H., Taylor, J. R. M. (2006). Vertical-axis tidal-current generators and the Pentland Firth. *IMechE Journal of Power and Energy*. **221**, 181-199.

[2] Creech, A. C. W., Fruh, W-G., Maguire, A. E. (2015). Simulations of an offshore wind farm using large-eddy simulation and a torque-controlled actuator disc model. *Surveys in Geophysics*. **36(3)**, 427 - 481.

[3] Creech, A. C. W., Borthwick, A. G. L., Ingram, D. (2017). Effects of support structures in an LES actuator line model of a tidal turbine with contra-rotating rotors. *Energies*. **10**, 726.

[4] Creech, A. C. W. (2017). GitHub source code repository for Wind And Tidal Turbine Embedded Simulator (WATTES). Available online: https://github.com/wattes.

[5] Troldborg, N. (2008). Actuator line modeling of wind turbine wakes. *Mechanical Engineering*.

[6] LeBlanc, B. P., Ferreira, C. S. (2018). Experimental determination of thrust loading of a 2-bladed vertical axis wind turbine. *Journal of Physics: Conf. Series* **1037**(2018) 022043.

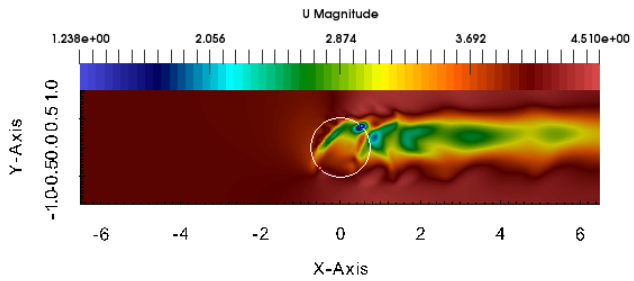


Fig. 1. Horizontal slice through instantaneous velocity field of a rotating VAT, with blade positions marked by crosses at around 130° and 310° respectively.

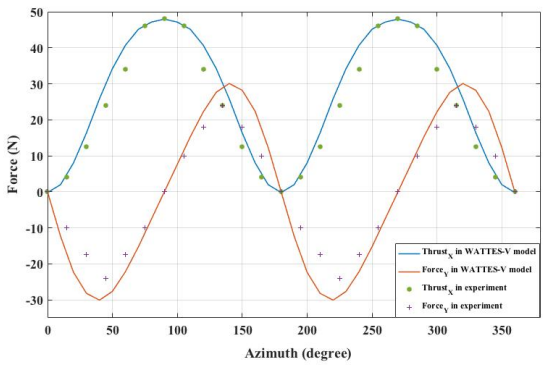


Fig. 2. Comparison between measured and predicted thrust and lateral forces for a flow speed of 4.01 m/s and a TSR of 3.7.

# 7th Oxford Tidal Energy Workshop (OTE 2019)

## Participants

| | |
|---|---|
| Tom Adcock | University of Oxford |
| Mohammed Alaa Almoghayer | Heriot-Watt University |
| Mohamad Hasif Bin Osman | University of Oxford |
| Paul Bonar | University of Edinburgh |
| Mitchell Borg | University of Strathclyde |
| Abdessalem Bouferrouk | University of the West of England |
| Byron Byrne | University of Oxford |
| Bowen Cao | University of Oxford |
| Michael Case | HR Wallingford |
| Lei Chen | University of Oxford |
| Xiaosheng Chen | Loughborough University |
| Vincent Clary | LEGI |
| Daniel Coles | SIMEC Atlantis Energy |
| Andres Cura Hochbaum | Technical University Berlin |
| Pierre-Luc Delafin | LEGI |
| Matt Edmunds | Swansea University |
| Steven Ettema | University of Oxford |
| Ahmad Firdaus | University of Oxford |
| Zoe Goss | Imperial College London |
| Guy Houlsby | University of Oxford |
| Jack Hughes | Swansea University |
| Wei Kang | University of Manchester |
| Monika Kreitmair | University of Edinburgh |
| Thomas Lake | Swansea University |
| Lun Ma | Cranfield University |
| Qian Ma | University of Oxford |
| Lucas Mackie | Imperial College London |
| Thierry Maitre | Grenoble-INP/LEGI |
| Marinos Manolesos | Swansea University |
| Ian Masters | Swansea University |
| James McNaughton | University of Oxford |

| | |
|---|---|
| Hannah Mullings | University of Manchester |
| Chantel Niebuhr | University of Pretoria |
| Takafumi Nishino | University of Oxford |
| Pablo Ouro | Cardiff University |
| Mohammad Rafiei | CNR-INM |
| Ed Ransley | Plymouth University |
| Yajun Ren | University of Edinburgh |
| Simon Reynolds | University of Edinburgh |
| Elie Ronge | Mott MacDonald |
| Kate Rossington | HR Wallingford |
| Zohreh Sarichloo | CNR-INM |
| Andrea Schnabl | University of Oxford |
| Qihu Sheng | Harbin Engineering University |
| Robert Shuker | Shuker & Sons |
| Richard Simons | UCL |
| Sophie Smith | Imperial College London |
| Tim Stallard | University of Manchester |
| Michael Togneri | Swansea University |
| Selahattin Ucuzcu | US Engineering & Consulting C. Ltd. |
| Merel Verbeek | Delft University of Technology |
| Christopher Vogel | University of Oxford |
| Simon Waldman | |
| Yinan Wang | University of Warwick |
| Richard Willden | University of Oxford |
| Aidan Wimshurst | Frazer-Nash Consultancy |
| David Kevin Woolf | Heriot-Watt University |
| Mohammad Yousef | University of Edinburgh |
| Ruiwen Zhao | University of Edinburgh |
| Binzhen Zhao | Harbin Engineering University |
| Federico Zilic de Arcos | University of Oxford |